



OPEN ACCESS

Original research

The human liver microenvironment shapes the homing and function of CD4⁺ T-cell populations

Benjamin G Wiggins ^{1,2,3}, Laura J Pallett ², Xiaoyan Li,^{1,4} Scott P Davies,^{1,3} Oliver E Amin,² Upkar S Gill,⁵ Stephanie Kucykowicz,² Arzoo M Patel,^{1,3} Konstantinos Aliazis,^{1,3} Yuxin S Liu,^{1,3} Gary M Reynolds,^{1,3} Brian R Davidson,⁶ Amir Gander,⁷ Tu Vinh Luong,⁸ Gideon M Hirschfield,^{3,9} Patrick T F Kennedy ⁵, Yuehua Huang,^{10,11} Mala K Maini,¹² Zania Stamataki ³

► Additional supplemental material is published online only. To view, please visit the journal online (<http://dx.doi.org/10.1136/gutjnl-2020-323771>).

For numbered affiliations see end of article.

Correspondence to

Dr Zania Stamataki, Centre for Liver and Gastrointestinal Research, University of Birmingham, Birmingham B15 2TT, UK; z.stamataki@bham.ac.uk and Professor Mala K Maini, Institute of Immunity and Transplantation, Division of Infection and Immunity, University College London, London, UK; m.maini@ucl.ac.uk

BGW, LJP and XL are joint first authors.

YH, MKM and ZS are joint senior authors.

Received 9 December 2020
Accepted 19 August 2021



© Author(s) (or their employer(s)) 2021. Re-use permitted under CC BY. Published by BMJ.

To cite: Wiggins BG, Pallett LJ, Li X, et al. *Gut* Epub ahead of print: [please include Day Month Year]. doi:10.1136/gutjnl-2020-323771

ABSTRACT

Objective Tissue-resident memory T cells (T_{RM}) are vital immune sentinels that provide protective immunity. While hepatic CD8⁺ T_{RM} have been well described, little is known about the location, phenotype and function of CD4⁺ T_{RM} .

Design We used multiparametric flow cytometry, histological assessment and novel human tissue coculture systems to interrogate the ex vivo phenotype, function and generation of the intrahepatic CD4⁺ T-cell compartment. We also used leukocytes isolated from human leukocyte antigen (HLA)-disparate liver allografts to assess long-term retention.

Results Hepatic CD4⁺ T cells were delineated into three distinct populations based on CD69 expression: CD69⁻, CD69^{INT} and CD69^{HI}. CD69^{HI}CD4⁺ cells were identified as tissue-resident CD4⁺ T cells on the basis of their exclusion from the circulation, phenotypical profile (CXCR6⁺CD49a⁺S1PR1⁻PD-1⁺) and long-term persistence within the pool of donor-derived leukocytes in HLA-disparate liver allografts. CD69^{HI}CD4⁺ T cells produced robust type 1 polyfunctional cytokine responses on stimulation. Conversely, CD69^{INT}CD4⁺ T cells represented a more heterogenous population containing cells with a more activated phenotype, a distinct chemokine receptor profile (CX₃CR1⁺CXCR3⁺CXCR1⁺) and a bias towards interleukin-4 production. While CD69^{INT}CD4⁺ T cells could be found in the circulation and lymph nodes, these cells also formed part of the long-term resident pool, persisting in HLA-mismatched allografts. Notably, frequencies of CD69^{INT}CD4⁺ T cells correlated with necroinflammatory scores in chronic hepatitis B infection. Finally, we demonstrated that interaction with hepatic epithelia was sufficient to generate CD69^{INT}CD4⁺ T cells, while additional signals from the liver microenvironment were required to generate liver-resident CD69^{HI}CD4⁺ T cells.

Conclusions High and intermediate CD69 expressions mark human hepatic CD4⁺ T_{RM} and a novel functionally distinct recirculating population, respectively, both shaped by the liver microenvironment to achieve diverse immunosurveillance.

INTRODUCTION

Tissue-resident memory T cells (T_{RM}) are a non-recirculating population that are critical in front-line adaptive immunity. Strategically positioned within tissues, these cells react to pathogen re-exposure more efficiently than circulating memory

Significance of this study

What is already known on this subject?

- Tissue-resident memory CD4⁺ and CD8⁺ T cells are important front-line immune sentinels in many human tissues.
- The human liver has been shown to contain long-lived tissue-resident CD8⁺ T cells that are capable of rapid effector function.
- Liver-resident CD4⁺ T cells remain uncharacterised, and their contribution to health and disease has not yet been studied.

What are the new findings?

- CD69 expression identifies three phenotypically and functionally distinct intrahepatic CD4⁺ T-cell populations: CD69⁻CD4⁺, CD69^{INT}CD4⁺ and CD69^{HI}CD4⁺.
- CD69^{HI}CD4⁺ T cells represent a long-lived liver-resident population that expresses classical retention markers, occupies sinusoidal and periportal niches, and is maintained in a resting and restrained state.
- CD69^{INT} marks a population containing both resident and recirculating T cells with differential chemokine and activation profiles.
- CD69^{HI}CD4⁺ T cells produce robust T_H1 cytokine responses, while CD69^{INT}CD4⁺ T cells favour the production of interleukin-4 on short-term T-cell receptor engagement.
- The frequency of CD69^{INT}CD4⁺ T cells correlates with necroinflammatory scores in patients with chronic hepatitis B infection.
- Novel autologous liver slice coculture models promote the differentiation of both CD69^{INT}CD4⁺ and CD69^{HI}CD4⁺ cells from blood, but hepatic epithelia were sufficient to induce the CD69^{INT}CD4⁺ phenotype.

subsets.¹ This function is mediated directly and by employing an innate-like ‘sensing and alarm’ strategy to enable recruitment and activation of other effector cells.^{2,3} Human T_{RM} have now been identified in many organs^{1,4,5} and differ substantially from their circulating counterparts in phenotype,⁶ function,^{7,8} metabolism,⁹ maintenance

Significance of this study

How might it impact on clinical practice in the foreseeable future?

- ▶ Our study identifies distinct intrahepatic CD4⁺ T cells not detectable in the blood, underscoring the need for continued sampling of the liver.
- ▶ An understanding of the differential functionality of CD69^{HI}CD4⁺ and CD69^{INT}CD4⁺ T cells compartmentalised at the site of pathology has important implications for current intensive efforts to develop immunotherapies for liver diseases.
- ▶ The capacity of liver-derived signals to allow *in vitro* recapitulation of tissue-resident CD4⁺ T cells could be exploited for therapeutic targeting.

requirements¹¹ and responsiveness to stimuli.¹² Expression of tissue retention molecules CD69, CD103 and CD49a and a lack of tissue egress markers including CCR7 and sphingosine-1-phosphate receptor 1 (S1PR1) define T_{RM}.¹³ Of these, CD69 is particularly important as a marker preserved on CD4⁺ and CD8⁺ T_{RM} in all tissues,¹⁴ and separation through expression of this molecule alone has recently been used to define a human T_{RM} transcriptome with strong fidelity to more established murine T_{RM} profiles.^{13 15}

Recently, Pallett *et al* identified intrahepatic CD8⁺ T_{RM} (CD69⁺CD103⁺CXCR6⁺CXCR3⁺PD-1⁺ (PD-1 – programmed cell death protein-1)), capable of robust interleukin (IL)-2 production, associated with viral control in the liver of HBV-infected individuals.⁵ However, little is known about CD4⁺ T_{RM} and how the liver shapes their biology. In one study, Wong *et al* outlined distinct activation, differentiation and homing receptor profiles of liver perfusate CD4⁺ T cells as part of a multiorgan mapping study,¹⁶ supporting the possibility of a liver-resident CD4⁺ T-cell population.

Here, we provide the first comprehensive phenotypical and functional analysis of intrahepatic CD4⁺ T_{RM} in the human liver. We identified two distinct populations of CD69-expressing intrahepatic CD4⁺ T cells: CD69^{HI} and CD69^{INT}. CD69^{HI}CD4⁺ T cells within the human liver had prototypical hallmarks of tissue residency, including high expression of retention markers, exclusion from the circulation and rapid multifunctional type 1 cytokine production on stimulation. We also report a novel population of intrahepatic CD69^{INT}CD4⁺ T cells characterised by a unique chemokine receptor profile (CD69^{INT}CX₃CR1⁺CXCR3⁺CXCR1⁺). CD69^{INT}CD4⁺ cells retained the ability to recirculate and on stimulation produced the T_H2 cytokine IL-4. The frequency of these CD69^{INT}CD4⁺ T cells also correlated with necroinflammatory scores in patients with chronic hepatitis B. Finally, we demonstrated that contact with hepatic epithelia drives the CD69^{INT}CD4⁺ phenotype, while CD69^{HI}CD4⁺ cells required additional signals from the liver microenvironment.

MATERIALS AND METHODS

Patient samples and immune cell isolation

Blood, liver and lymph node (LN) samples were obtained from centre A, the Queen Elizabeth Hospital, Birmingham (references 06/Q2702/61 and 06/Q2708/11). Blood, liver (resections, biopsies, fine needle aspirates, HLA-mismatched explants), gut, spleen and LN samples from centre B were obtained from either the Royal Free Hospital, London (references 16/WA/0289, 11/WA/0077, 11/H0720/4 (RIPCOLT clinical trial number 8191)

or 11/LO/0421) or Royal London Hospital, Barts Health NHS Trust (references P/01/023, 16/LO/1699 or 17/LO0266). Immune cells were isolated from tissues/blood through tissue digestion and density centrifugation (see online supplemental experimental methods). See online supplemental table 1 for full patient details.

Flow cytometry

For surface staining, cells were incubated with fluorescence-conjugated antibodies on ice for 20–30 min. For intracellular staining, cells were either fixed with 1% formaldehyde (Sigma-Aldrich) for 15 min, permeabilised with 0.1% Saponin (Sigma-Aldrich) and stained with relevant antibodies in 0.1% saponin (30 min, 20°C), or fixed and permeabilised with Cytofix/Cytoperm (BD Bioscience) or FoxP3 Buffer Set (BD Bioscience) according to the manufacturer's instructions, and stained in 0.1% saponin. Dead intrahepatic lymphocytes (IHLs) were identified and excluded using either a fixable live/dead dye (Thermo Fisher) for all centre B samples or zombie dyes (Biolegend) for all cultured centre A samples. Samples were analysed on an ADP CyAn flow cytometer running Summit software (Beckman Coulter, centre A) or LSRII or X20 flow cytometers running FACSDiva software (BD Bioscience) for samples from centre B (see online supplemental table 2 for the list of antibodies used and online supplemental figure 1 for gating strategies). CD69⁻ and CD69^{INT} populations were distinguished using isotype-matched controls, in combination with peripheral blood staining to determine CD69^{INT} versus CD69^{HI} gate positions.

Immunofluorescence

Formalin-fixed paraffin-embedded 3 µm liver sections were deparaffinised with xylene, rehydrated with 99% industrial denatured alcohol and underwent antigen retrieval by microwaving in Tris-based antigen-unmasking solution (Vector Labs). Slides were washed with TBS +0.1% Tween (TBST) and 2× casein solution (Vector Labs) was added for 10 min, before 1-hour incubation with primary antibodies diluted in TBST. For antibodies used, see online supplemental experimental procedures. Following three washes with TBST, secondary antibodies were applied for 1 hour in TBST; autofluorescence was quenched with the TrueVIEW autofluorescence quenching kit (Vector Labs); and tissues were mounted with VECTASHIELD Vibrance Antifade Mounting Medium with DAPI (4',6-diamidino-2-phenylindole, Vector Labs). Tissues were imaged using the Zeiss LSM 880 confocal microscope (Carl Zeiss) equipped with a ×63 water immersion objective.

T-cell stimulation for assessment of cytokine production

Peripheral blood mononuclear cells (PBMCs) and IHLs were first stained for surface antigens then cultured alone, with 1:1 ratio of anti-CD3/CD28 beads (Dynabeads, ThermoFisher), or 50 ng/mL phorbol 12-myristate 13-acetate (PMA) and 1 µM ionomycin (both Sigma Aldrich, UK), all with 10 µg/mL Brefeldin A (Sigma Aldrich). For culture and media details, see online supplemental experimental procedures.

CD4⁺ T-cell isolation and cell culture

CD4⁺ T cells were isolated from PBMCs with the EasySep human CD4⁺ T-cell enrichment kit, or EasySep naïve/memory human CD4⁺ T-cell enrichment kits (all StemCell Technologies). T cells/PBMCs were cultured with hepatic epithelial cell lines (Huh-7, HepG2 and Hep3B), hepatic stellate cell line LX-2, primary hepatic sinusoidal endothelial cells (HSECs) and primary biliary

epithelial cells (BECs). Primary BEC and HSEC were isolated in-house as previously described.^{17, 18} For media details, see online supplemental experimental procedures. 1×10^6 PBMCs/T-cells were added per well and cultured for up to 7 days. For transwell separation experiments, T cells were added to the top of the 0.4 μm pore transwell insert, separated from hepatic cells at the bottom of the 24-well plate.

Liver slice cultures

Precision-cut liver slices of 2 mm were prepared using a TruSlice tissue slicer (CellPath) and were cultured in complete Dulbecco's Modified Eagle Medium (DMEM) with 2% foetal bovine serum (FBS) in 48-well plates. Autologous total PBMCs were added in T-cell media (1×10^6 /well), and plates were cultured for 5 hours at 37°C before PBMC harvest and were used in downstream assays.

Data analysis and statistics

All flow cytometry data were analysed using FlowJo V.9–10 (FlowJo LLC). Statistical testing was applied in Prism V.8 (GraphPad). Median average values and non-parametric testing were used throughout.

RESULTS

CD69 expression distinguishes three intrahepatic CD4⁺ T-cell populations with differential homing potentials

To identify intrahepatic CD4⁺ T_{RM}, we analysed CD69 expression in over 160 liver samples from two research centres. Three intrahepatic CD4⁺ T-cell phenotypes were identified: CD69⁻, CD69^{INT} and CD69^{HI} (figure 1A). CD69^{HI}CD4⁺ cells were negligible in blood, while CD69^{INT}CD4⁺ T cells were detected in both intrahepatic and peripheral pools (figure 1B). In the liver, CD69^{HI}CD4⁺ T cells displayed striking concordance with a residency-associated profile (CD49a⁺CX₃CR6⁺S1PR1⁻CX₃CR1⁻) (figure 1C). By contrast, CD69^{INT}CD4⁺ T cells retained expression of the tissue egress marker S1PR1 and fractalkine receptor CX₃CR1, which is associated with migratory T cells,^{13, 19, 20} as well as the strongest expression of parenchymal homing receptors CXCR3 and CXCR1.²¹ Hepatic CD69^{INT}CD4⁺ T cells expressed less CD49a and CXCR6 than CD69^{HI}CD4⁺ T cells, although these residence markers were all expressed to a higher extent than on the CD69⁻CD4⁺ T cells.

In keeping with their association with residence, fine-needle aspirate (FNA) samples (that sample more blood-derived than interstitial T cells compared with biopsies²²) showed a more marked reduction in the frequency of CD69^{HI}CD4⁺ than CD69^{INT}CD4⁺ T cells compared with matched liver tissue obtained by biopsy (online supplemental figure 2A). Similarly, of the three populations, only CD69^{HI}CD4⁺ T cells were enriched for an effector memory phenotype—a prerequisite for T_{RM} cells (online supplemental figure 2B). Interestingly, more CD69^{INT}CD4⁺ T cells expressed a gut homing signature (CCR9, integrin $\alpha\beta 7$) than the other two CD69-expressing populations, suggestive of a potential wider enteric surveillance role (online supplemental figure 2C). Additional profiling revealed increased CCR5 expression on CD69^{HI}CD4⁺ T cells, higher expression of CCR6 on both CD69-expressing populations than CD69⁻CD4⁺ T cells and no differential CCR10 expression. The retention marker CD103 was expressed most on CD69^{HI}CD4⁺ T cells, although this frequency was low, as reported for other human resident CD4⁺ T-cell subsets (online supplemental figure 2C).⁴ Together, our data reveal two distinct CD69-expressing CD4⁺ T-cell populations in the human liver: CD69^{HI}CD4⁺ T

cells with the strongest T_{RM} profile and CD69^{INT}CD4⁺ T cells with differential homing potential.

Next, we assessed whether differential expression of CXCR6 and CX₃CR1 between the different intrahepatic CD4⁺ T-cell populations affected their hepatic distribution (online supplemental figure 3A). CD4⁺ T cells expressing either chemokine receptor were found throughout the liver—in both portal and central areas, in fibrotic tracts and throughout the parenchyma where they likely play a crucial role in the immunosurveillance of hepatocytes (figure 1D,E, and online supplemental figure 3A–C). CXCR6⁺CD4⁺ T cells (enriched for the CD69^{HI}CD4⁺ T-cell population) were found more frequently in association with bile ducts (figure 1F), in keeping with the role of this receptor in biliary homing.²³

High CD69 expression marks a CD4⁺ T-cell population capable of long-term residence within the liver

To ascertain which population was strictly resident in the human liver, we examined HLA-mismatched allograft samples explanted up to a decade after initial transplantation.²⁴ In our recent study, we showed that in all cases, a small pool of long-lived, donor-derived CD4⁺ T cells were detected by staining with HLA-specific antibodies.²⁴ No donor-derived CD4⁺ T cells were detected in the blood, confirming that donor-derived cells and their progeny were maintained locally in the liver allograft.²⁴ Re-examining the CD4⁺ T-cell fraction from donor and recipient pools, we observed that CD69^{HI}CD4⁺ T cells were significantly enriched in the persisting, donor-derived fraction, establishing these cells as T_{RM} (figure 2A). By contrast, CD69⁻CD4⁺ T cells comprised a negligible fraction of the long-lived donor-derived T cells. Interestingly, however, a population of CD69^{INT}CD4⁺ T cells was detected in the donor-derived compartment in all cases, suggestive of the long-term retention of some of these cells. Examining the recipient-derived CD4⁺ T cells infiltrating the allograft, we found these to be capable of acquiring both a CD69^{HI}CXCR6^{HI} and a CD69^{INT}CXCR6^{LO} phenotype, suggesting that infiltrating T cells are shaped by the hepatic microenvironment (figure 2B). By contrast, recipient CD4⁺ T cells within the allograft only showed a subtle increase in CXCR3 compared with their circulating counterparts, expressing much less than the donor-derived CD69^{HI}CD4⁺ and CD69^{INT}CD4⁺ T cells, suggesting CXCR3 is less easily imprinted on liver infiltration (figure 2B). Donor-derived CD69^{HI}CD4⁺ T cells contained a greater representation of dual CXCR6⁺CXCR3⁺-expressing cells than their recipient-derived counterparts, while the CXCR6⁻CXCR3⁺ was most enriched on the donor-derived CD69^{INT}CD4⁺ T-cell population (figure 2C). This suggests expression of both markers is important in long-term retention of CD69^{HI}CD4⁺ T cells, with CD69^{INT}CD4⁺ T cells more reliant on CXCR3 alone.

Reasoning that expression of tissue egress markers S1PR1 and CX₃CR1 would imbue CD69^{INT}CD4⁺ T cells with the ability to recirculate through lymphatics, we assessed the make-up of matched liver and liver-draining hepatic hilar LN (hepatic lymph node (hLN), figure 2D) and distal non-hLN (figure 2E). Both CD69^{INT}CD4⁺ and CD69^{HI}CD4⁺ T cells were present in LNs, supporting this possibility. While donor-matched liver and hLN CD69^{HI}CD4⁺ T cells were phenotypically similar, reflective of a common residency signature, CD69^{INT}CD4⁺ and CD69⁻CD4⁺ cells in hLNs differed substantially from their liver equivalents in their chemokine receptor profile (subsets in hLNs enriched for CXCR3, but depleted for CX₃CR1, CXCR1 and CCR9 expression; figure 2F). Furthermore, CD69^{HI}CD4⁺ and CD69^{INT}CD4⁺ were detectable not only in the liver and LNs but also in the

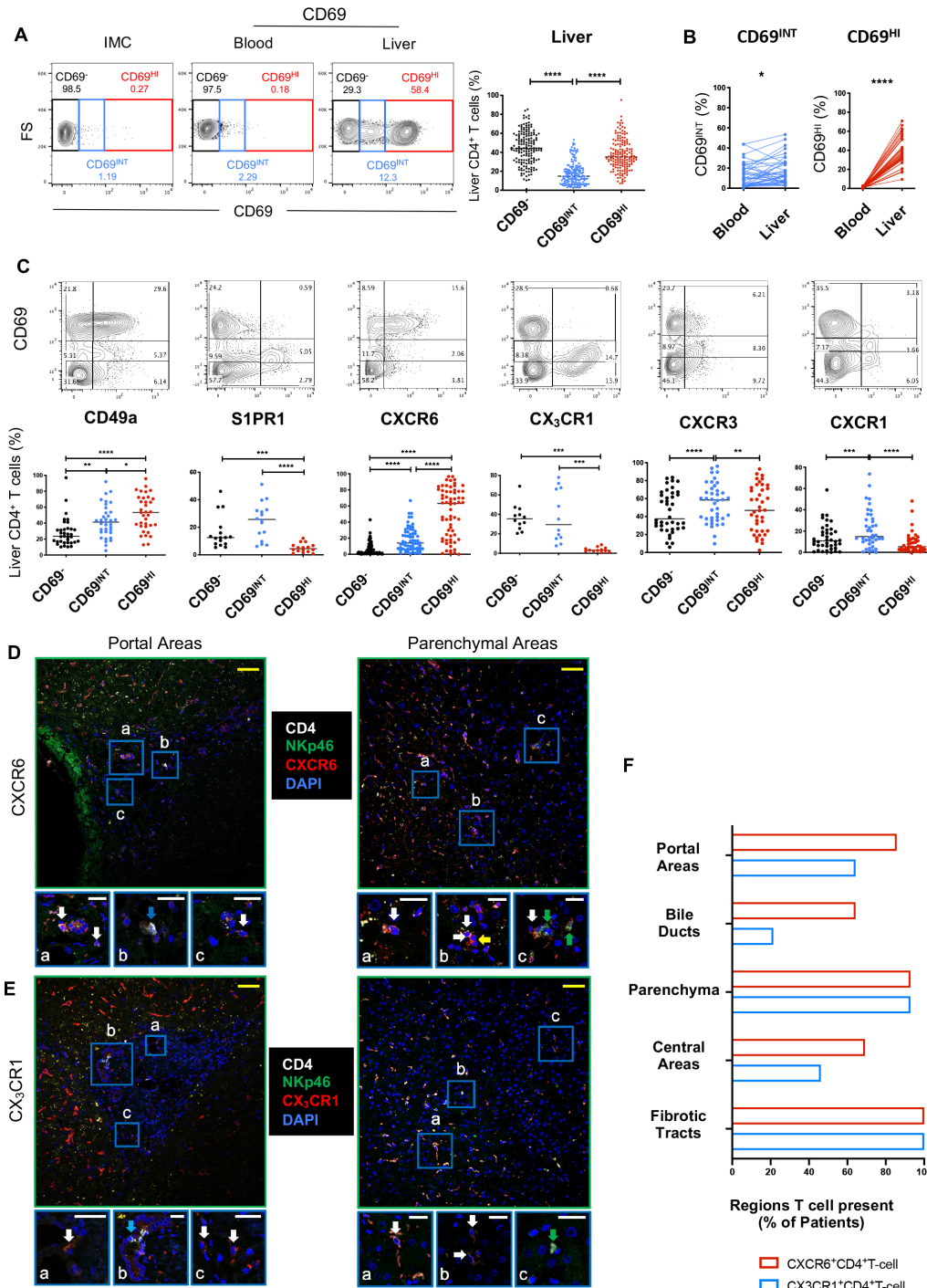


Figure 1 CD69 expression distinguishes three intrahepatic CD4⁺ T-cell populations with differential homing potentials. (A) Gating strategy showing CD69⁻, CD69^{INT} and CD69^{HI} populations. Representative flow cytometry plot for CD4⁺ T-cell distribution in blood and liver, and summary data showing % CD4⁺ T cells in IHL from two independent centres (n=162). Isotype-matched controls were used to set CD69⁻ gates. (B) % CD69-expressing T-cell populations in paired blood and liver (n=39). (C) Expression of key homing and retention markers on CD69-expressing CD4⁺ T cells (% of total CD4⁺ T cells). Images depicting localisation of CXCR6⁺ CD4⁺ T cells (D) or CX₃CR1⁺ CD4⁺ T cells (E) in portal and parenchymal areas of human livers (representative of n=14 livers (5 control, 4 patients with HBV and 5 patients with PBC)). Sections stained for CD4, Nkp46, DAPI and chemokine receptor indicated. Cells of interest expressed both the chemokine receptor and CD4 and lacked NK cell marker Nkp46. Areas of interest (A–C) shown at higher magnification below each main image. White arrows: cell of interest, green arrows: Nkp46⁺ cell, yellow arrow: chemokine receptor⁺ CD4⁻ cell, blue arrows: CD4⁺ Nkp46⁻ CXCR6⁻ cells (D) or CD4⁺ Nkp46⁻ CX₃CR1⁻ cells (E). Yellow scale bars: 50 µm, white scale bars: 20 µm. (F) Cumulative scoring of the presence of each cell of interest within different liver regions. Cells of interest were scored as present in specific areas if at least three cells were present within each region. Plot shows the % of each region that contained cells of interest (n=14, as above; fibrotic tracts in non-control livers only, n=9). Cells were classed as present in portal regions and central regions if they were identified within 50 µm of their respective vasculature. Association with bile ducts was scored if cells were making direct contact. Statistical comparisons by Freidman tests with Dunn's multiple tests (A,C); Wilcoxon matched-pair, signed-rank tests (B). p < 0.05 (*), < 0.01 (**), < 0.001 (***), < 0.0001 (****) FS, forward scatter; IHL, intrahepatic lymphocyte; IMC, isotype-matched control; NK, natural killer; PBC, primary biliary cholangitis.

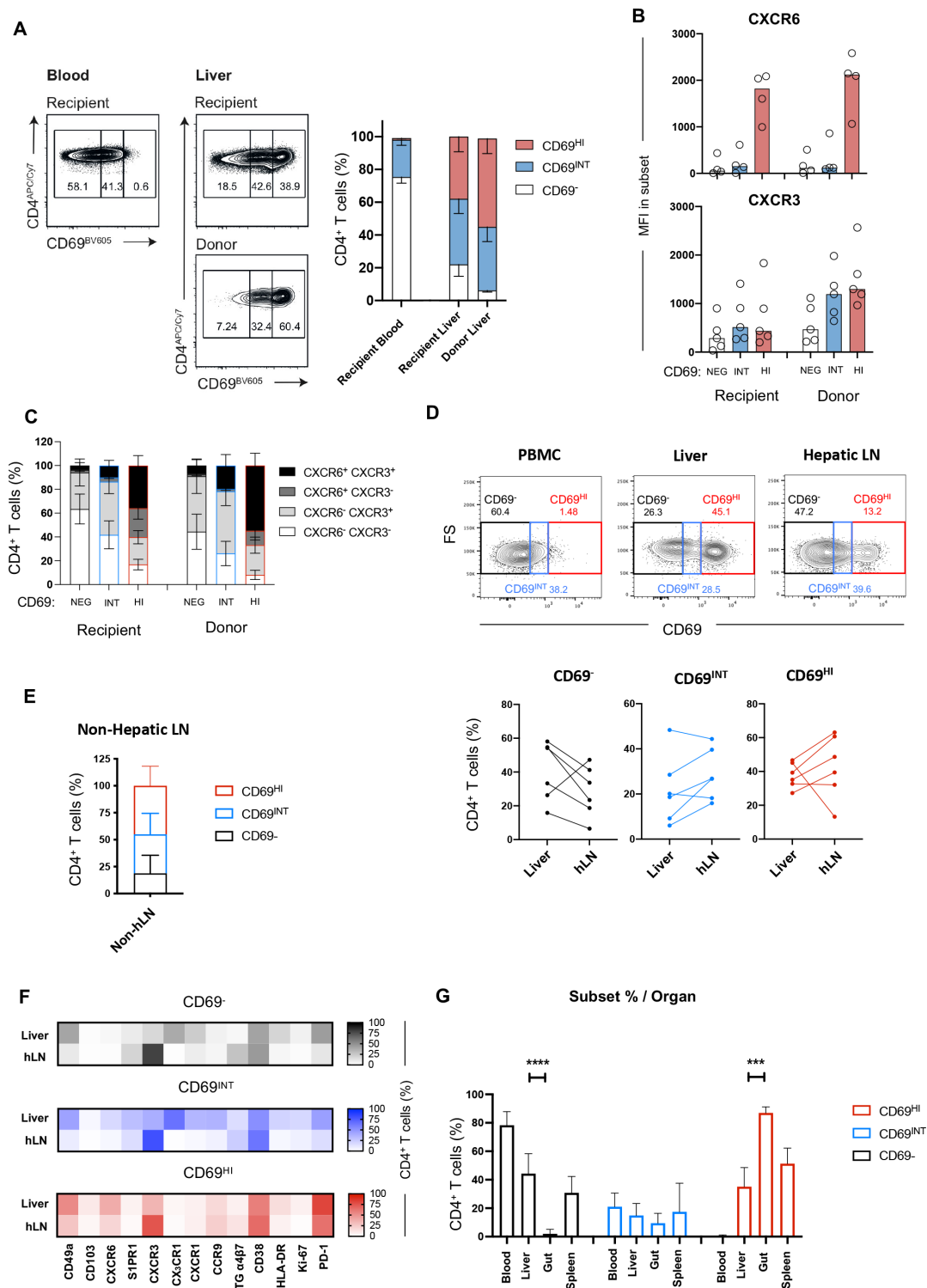


Figure 2 High CD69 expression marks a CD4⁺ T-cell population capable of long-term residence within the liver. (A) HLA-mismatched allograft sampling allows assessment of resident T cells. Donor-derived T cells are distinguished from recipient-derived T cells through HLA staining. Example distributions of CD69⁻, CD69^{INT} and CD69^{HI} cells in recipient and donor pools of liver and blood samples, and combined data across five patient samples. (B) MFI of CXCR6 and CXCR3 expressions in the three populations in donor and recipient pools. (C) Breakdown of CXCR3/CXCR6 coexpression patterns in different donor and recipient subpopulations (n=4). (D) Staining and combined data showing population distribution from liver (n=6), hepatic LNs (n=6) and non-hepatic (mesenteric) LNs (n=6). Example plots show hLN, PBMC and liver as gating controls. (E) Subset breakdown in distal non-hLNs. (F) Heatmap of % marker expression in CD69⁻ (top), CD69^{INT} (middle) and CD69^{HI} (bottom) from matched liver and hLN samples. CD103, n=6; CD49a, n=5; CXCR6 and HLA-DR, n=4; CXCR3, CXCR1, PD-1 and CD38, n=3; S1PR1, CCR9, integrin α 4 β 7 and Ki-67, n=2; CX₃CR1, n=1. (G) Frequency of CD69⁻, CD69^{INT} and CD69^{HI} CD4⁺ T cells in blood (n=103), liver (n=118), gut (n=6) and spleen (n=4) samples. Statistical comparisons on paired populations by Wilcoxon matched-pair, signed-rank tests (A–D,F), and Kruskal-Wallis tests with dunn's post hoc tests on liver, gut and spleen samples within each CD4⁺ T-cell subset (G). HI, high; hLN, hepatic lymph node; INT, intermediate; LN, lymph node; MFI, Median fluorescence intensity, NEG, negative.

gut, where CD69^{HI}CD4⁺ predominates, and in spleen samples (figure 2G).

Thus, while the properties of long-lived tissue enrichment and absence from the peripheral circulation mean CD69^{HI}CD4⁺ T cells comply with a tissue-resident definition, CD69^{INT}CD4⁺ T cells may represent a population with a context-dependent capacity for liver occupancy and egress.

CD69^{HI}CD4⁺ T_{RM} demonstrates a restrained, resting phenotype, while CD69^{INT}CD4⁺ T cells exhibit features of activation

Alongside a tissue-residence marker, CD69 has been used as an indicator of early lymphocyte activation.²⁵ Therefore, we examined the activation status of the three hepatic

CD4⁺ T-cell populations. Intriguingly, the extent of cellular activation did not correlate with levels of CD69 expression; CD69^{INT}CD4⁺ T cells were enriched for activation markers CD38 and HLA-DR, expressing more CD38 than CD69⁻CD4⁺ T cells, and more HLA-DR than CD69^{HI}CD4⁺ T cells (figure 3A). Consistent with recent activation in vivo, the CD69^{INT}CD4⁺ T-cell population also expressed more Ki67 than their CD69^{HI}CD4⁺ T-cell counterparts (figure 3B). Regulatory T cells (T_{REG}, CD4⁺CD25^{HI}CD127^{LO}) were not significantly enriched in any intrahepatic CD4⁺ population, irrespective of CD69 expression, and T_{REG} functional markers cytotoxic T lymphocyte-associated protein-4 (CTLA4) and CD39 were similarly expressed by both CD69-expressing

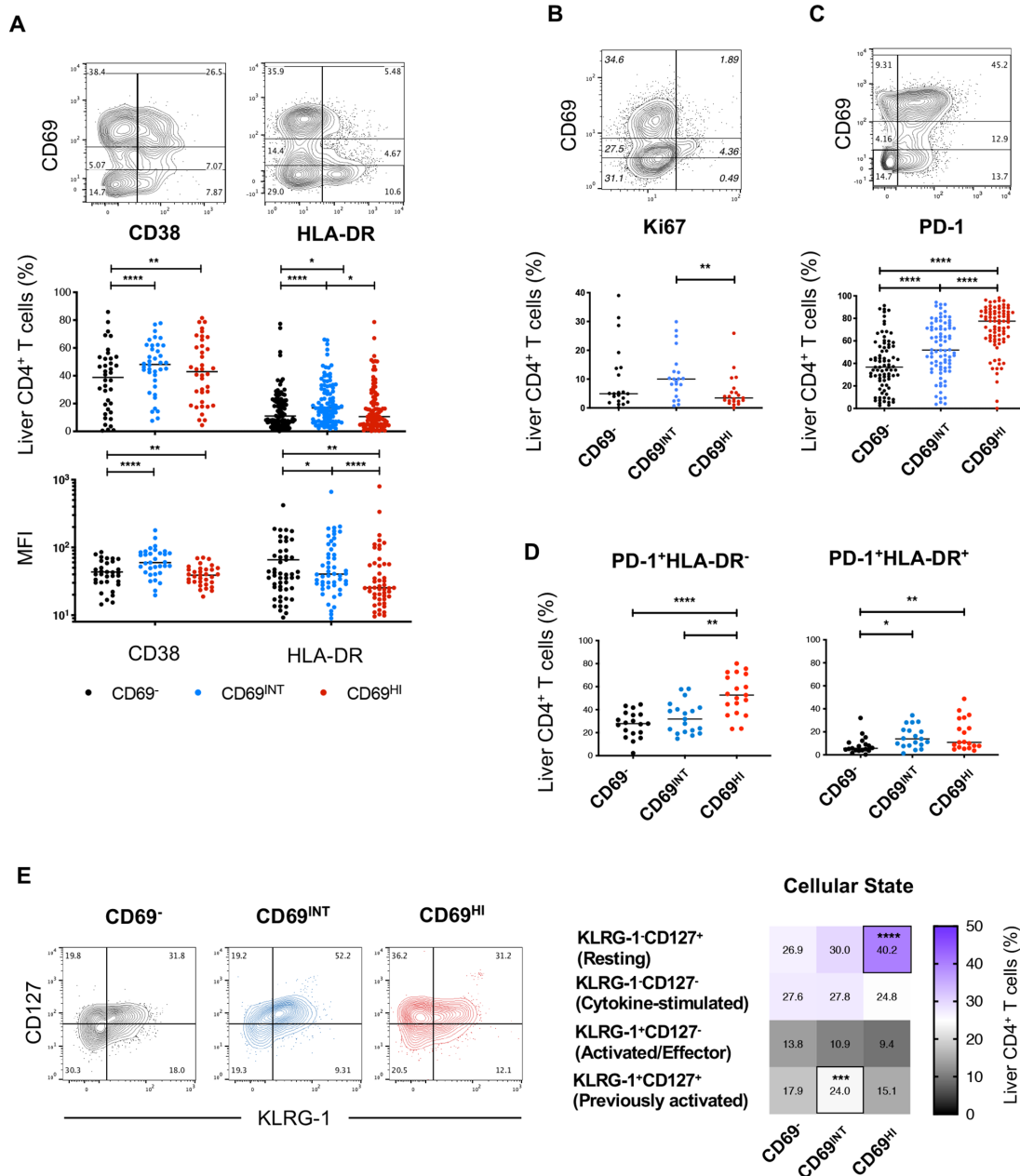


Figure 3 CD69^{HI}CD4⁺ T_{RM} demonstrate a restrained, resting phenotype, while CD69^{INT}CD4⁺ T cells exhibit features of activation. (A) % and MFI expression of CD38 and HLA-DR. % expression of (B) Ki-67 and (C) PD-1 expressions among the three CD4⁺ T-cell populations. (D) Subset representation among PD-1⁺HLA-DR⁻ and PD-1⁺HLA-DR⁺ designations (n=19). (E) Analysis of the four differentiation/cellular states based on KLRG-1 and CD127 expressions (n=41). Heatmap shows % expression of each designation. Freidman’s tests with Dunn’s multiple tests were used for statistical analysis (A–E) p < 0.05 (*), < 0.01 (**), < 0.001 (***), < 0.0001 (****). MFI, mean fluorescence intensity.

populations when compared with CD69⁻CD4⁺ T cells (online supplemental figure 4).

Another hallmark of human T_{RM} is the adoption of a self-restrained, resting state necessary to prevent inflammatory damage to residing tissues.^{5 13 15} Correspondingly, CD69^{HI}CD4⁺ T cells were enriched for PD-1, with CD69⁻CD4⁺ T cells displaying the lowest frequency (figure 3C). As PD-1 can also denote activation,²⁶ we assessed the coexpression of PD-1 and HLA-DR. The percentage of PD-1⁺HLA-DR⁻ cells were enriched within the CD69^{HI}CD4⁺ T-cell population, suggesting PD-1 upregulation in CD69^{HI}CD4⁺ T cells was not simply an activation phenomenon (figure 3D). To investigate cellular activation states in more detail, we also analysed coexpression patterns of killer cell lectin-like receptor-G1 (KLRG-1, a marker of antigen experience) and CD127, an indicator of common γ -chain cytokine sensitivity.^{27 28} As in human T_{RM} studies,²⁹ CD69^{HI}CD4⁺ T cells contained the most resting (KLRG-1⁻CD127⁺) cells, whereas CD69^{INT}CD4⁺ T cells were enriched for the previously activated (KLRG-1⁺CD127⁺) population (figure 3E).

These data illustrate differences in activation states between CD69^{HI}CD4⁺ and CD69^{INT}CD4⁺ T cells, with the former exhibiting a resting/restrained phenotype in keeping with their profile as liver T_{RM}, while the latter population displayed features consistent with recent activation.

Liver CD69^{HI}CD4⁺ and CD69^{INT}CD4⁺ T cells are skewed towards T_H1 and T_H2 functional profiles, respectively

CD4⁺ T_{RM} cells have a superior functional capacity to circulating T cells and mediate protection against a number of viral infections in multiple organs.^{1 15} To assess the functional potential of CD69^{HI}CD4⁺ T_{RM} and CD69^{INT}CD4⁺ T cells, intrahepatic leukocytes from a subset of livers were first prestained for CD69 expression to rule out stimulation-induced changes to CD69 expression and then were stimulated to assess their capacity for cytokine production. Following T-cell receptor (TCR) ligation with 5-hour anti-CD3/CD28 stimulation, more CD69^{HI}CD4⁺ T cells produced interferon gamma (IFN- γ) and IL-21 than any other population, and both CD69^{HI} and CD69^{INT}CD4⁺ T cells were enriched for IL-2, and tumour necrosis factor alpha (TNF- α) compared with their CD69⁻CD4⁺ counterparts (figure 4). Among the two CD69-expressing populations, CD69^{INT}CD4⁺ T cells expressed more IL-4, with no differential expression patterns noted for IL-17 or IL-10.

We also assessed the maximum functional capacity of these cells following stimulation with mitogens PMA and ionomycin, and the direct *ex vivo* cytokine levels produced without exogenous stimulation. Similar to anti-CD3/CD28 stimulation, IFN- γ and IL-21 were also highest in CD69^{HI}CD4⁺ T cells in PMA/ionomycin-stimulated conditions, and IL-4 was similarly enriched in CD69^{INT} versus CD69^{HI}CD4⁺ T cells (online supplemental figure 5A). This stimulation also demonstrated CD69^{HI}CD4⁺ T cells possessed the greatest potential to produce IL-2 and TNF- α and a higher potential than CD69⁻CD4⁺ T cells to produce IL-17. Importantly, in the absence of an exogenous stimulation, CD69^{INT}CD4⁺ T cells produced IL-4, and CD69^{HI}CD4⁺ T cells showed a small enrichment for IFN- γ and IL-21 production compared with CD69⁻CD4⁺T-cells (online supplemental figure 5B), perhaps reflecting recent *in vivo* stimulation. IL-10 was not enriched in any subset irrespective of stimulation, in line with the lack of an over-representation of a T_{REG} phenotype in either CD4⁺ T-cell subset (online supplemental figure 4).

Human T_{RM} from other organs are often polyfunctional, producing the cytokines IFN- γ , TNF- α and IL-2 simultaneously, a

property that equips these T cells for better pathogen control.³⁰⁻³⁴ Likewise, we observed an increase in IL-2⁺TNF- α ⁺IFN- γ ⁺ type 1 multifunctional cells in CD69^{HI}CD4⁺ T cells compared with CD69⁻CD4⁺ T cells, a feature not shared by CD69^{INT}CD4⁺ T cells (online supplemental figure 5C). Finally, assessment of CD4⁺ T-cell transcription factors revealed an increase in T-bet in CD69^{HI}CD4⁺ T cells in line with an enrichment for IFN- γ production, but we were unable to detect T_H2 transcription factor GATA-3 in hepatic CD4⁺ T cells (online supplemental figure 6). ROR γ t and FoxP3 were not differentially enriched in either CD69-expressing subset.

Taken together, CD69^{HI}CD4⁺ and CD69^{INT}CD4⁺ T cells are functionally distinct, with CD69^{HI}CD4⁺ T cells favouring IFN- γ and type 1 multifunctional responses, while CD69^{INT} expression predisposed CD4⁺ T cells to enhanced IL-4 production.

Increased CD69^{INT}CD4⁺ T-cell frequencies correlate with necroinflammation in chronic HBV infection (CHB)

Next, we stratified liver samples into CHB, autoimmune (autoimmune hepatitis, primary biliary cholangitis and primary sclerosing cholangitis), dietary-induced liver disease (alcoholic liver disease and non-alcoholic steatohepatitis) and control (healthy preimplant, healthy transplant rejections, non-tumour-associated colorectal cancer and hepatocellular carcinoma margins and cyst-free margins of polycystic liver disease tissue) groups to test for population enrichment across diseases. CD69^{HI}CD4⁺ T-cell frequencies showed a modest yet consistent reduction in patients with CHB compared with control livers, but no other disease-specific differences were observed (figure 5A). To test if activated CD69^{INT}CD4⁺ T cells correlated with disease progression, we analysed model for end-stage liver disease (MELD) scores (a commonly used metric to assess severity of non-viral chronic liver disease³⁵) in explanted livers from patients with chronic hepatitis. There was no correlation with either CD4⁺T-cell population and MELD score, irrespective of liver disease aetiology, potentially reflective of a putative role for these cells in both health and disease (figure 5B).

Progression to advanced fibrosis in CHB is highly heterogeneous, with the duration of infection and phase of disease contributing to this process.³⁶ When analysing patients with CHB by hepatitis B 'e' antigen (HBeAg) seropositivity, viraemia, or the extent of liver inflammation using serum alanine aminotransferase (ALT) concentrations,³⁶ we noted that CD69^{INT}CD4⁺ T-cell frequencies correlated weakly with serum HBV DNA (figure 5C). The presence of HBeAg or serum ALT did not correlate with any CD4⁺ T-cell population (online supplemental figure 7A–B). Combined analysis of these three metrics into the distinct clinical phases also revealed no subpopulation-linked association (online supplemental figure 7C).

In order to further assess any links between populations and degree of fibrosis, and ongoing necroinflammatory activity, we subcategorised the patients using the validated Ishak and Histology Activity Index-Necroinflammatory scoring systems.³⁷ Frequencies of CD69^{INT}CD4⁺ T cells and CD69^{HI}CD4⁺ T_{RM} cells did not correlate with the extent of fibrosis by Ishak scoring (figure 5D). However, CD69^{INT}CD4⁺ T cells were more frequently observed in patients with a higher intrahepatic necroinflammatory score (figure 5E). Together, these data suggest that activated CD69^{INT} cells may play a role in inflammatory processes of CHB.³⁸

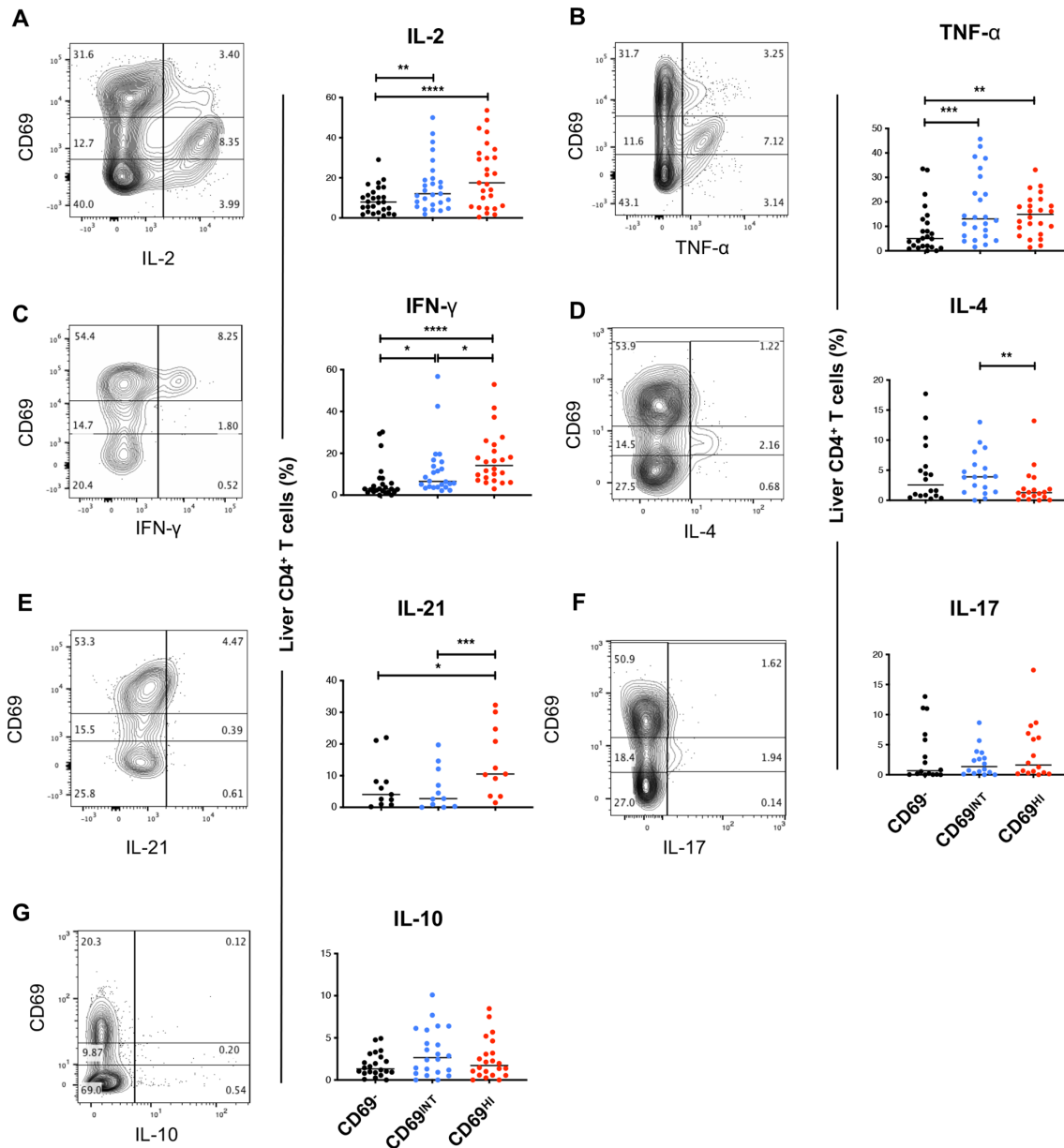


Figure 4 Liver CD69^{HI}CD4⁺ and CD69^{INT}CD4⁺ T cells are skewed towards T_H1 and T_H2 functional profiles, respectively. Each sample was stained with CD69 prior to stimulation to exclude effects of altered CD69 levels due to cellular activation. Representative flow plots and combined data of % expression of six prototypical T_H cytokines after 5 hours of stimulation of IHL with anti-CD3/CD28: (A) IL-2 (n=27), (B) TNF-α (n=24), (C) IFN-γ (n=24), (D) IL-4 (n=18), (E) IL-21 (n=11), (F) IL-17 (n=16), (G) IL-10 (n=22). See online supplemental table 4 for disease breakdowns. Freidman's tests with Dunn's multiple tests were used for statistical analysis (A–F). IFN-γ, interferon gamma; IHL, intrahepatic lymphocyte; IL, interleukin; TNF-α, tumour necrosis factor alpha.

CD69^{INT}CD4⁺ and CD69^{HI}CD4⁺ T-cells are differentially induced by the liver microenvironment

Finally, we sought to determine the origin of these distinct liver CD4⁺ T-cell populations by deconstructing the contribution of different hepatic cell types *in vitro*. To investigate the role of hepatic epithelia, we first cultured PBMC-derived CD4⁺ T cells with different hepatocyte cell lines (Huh-7, HepG2 and Hep3B); within 16 hours, we observed a clear induction of intermediate CD69 expression (figure 6A). By contrast, neither primary HSEC, primary BEC nor the hepatic stellate cell line, LX-2, was able to induce CD69 in the same time frame. However, primary BECs

were able to strongly promote the increase in CD69^{INT}CD4⁺ T cells from 72 hours, suggesting that sustained interaction with liver epithelia may be necessary for the generation of this population (online supplemental figure 8A–B). Hepatic epithelial-induced CD69 upregulation to an intermediate level was not simply a feature of their activation, as no concomitant upregulation of prototypical T-cell activation marker CD38 was seen, and conventional T cell activation with anti-CD3/CD28 led only to high CD69 expression (figure 6A–B). Mechanistically, this intermediate CD69 induction required direct T cell–epithelial cell contact, and was most efficient in memory CD4⁺ T cells (online

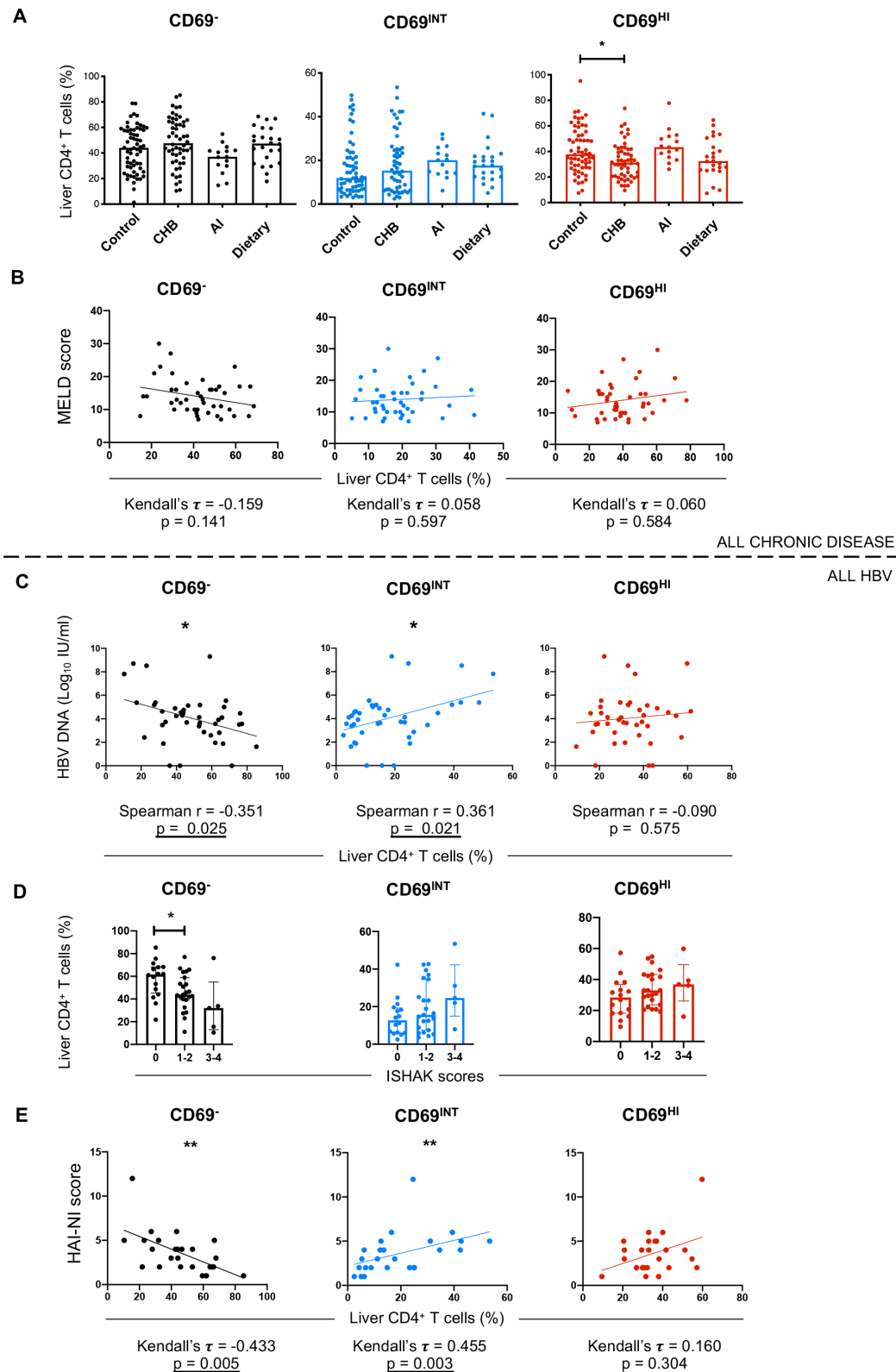


Figure 5 Increased CD69^{INT} CD4⁺ T-cell frequencies correlate with necroinflammation in CHB. (A) Representation of each population in control livers (n=62 (11 donor explant transplant rejections, 5 healthy tissue biopsies, 36 colorectal cancer margin liver explants, 8 HCC margin liver explants and 2 cyst-free areas of PLD explants)), patients with chronic HBV (CHB, n=54), autoimmune liver disease (n=15 (6 PBC, 8 PSC and 1 AIH)), and dietary liver disease (n=24 (16 ALD and 8 NASH)). (B) Correlation analysis of patient MELD scores versus % of each of the three subsets for all donors with end-stage liver disease from centre A. (C) HBV DNA, Ishak scoring (D) and HAI-NI scoring (E) plotted against % of each T-cell population in the HBV cohort. Correlation and p values reported for each plot. Statistical testing used: Kruskal-Wallis tests with Dunn's multiple post hoc tests (A,C), Kendall's tau rank correlation tests (B,E), Spearman's rank order correlation (C). AI, autoimmune; AIH, autoimmune hepatitis; ALD, alcoholic liver disease; CHB, chronic HBV infection; HAI-NI, Histology Activity Index-Necroinflammatory; HCC, hepatocellular carcinoma; NASH, non-alcoholic steatohepatitis; PBC, primary biliary cholangitis; PLD, polycystic liver disease; PSC, primary sclerosing cholangitis.

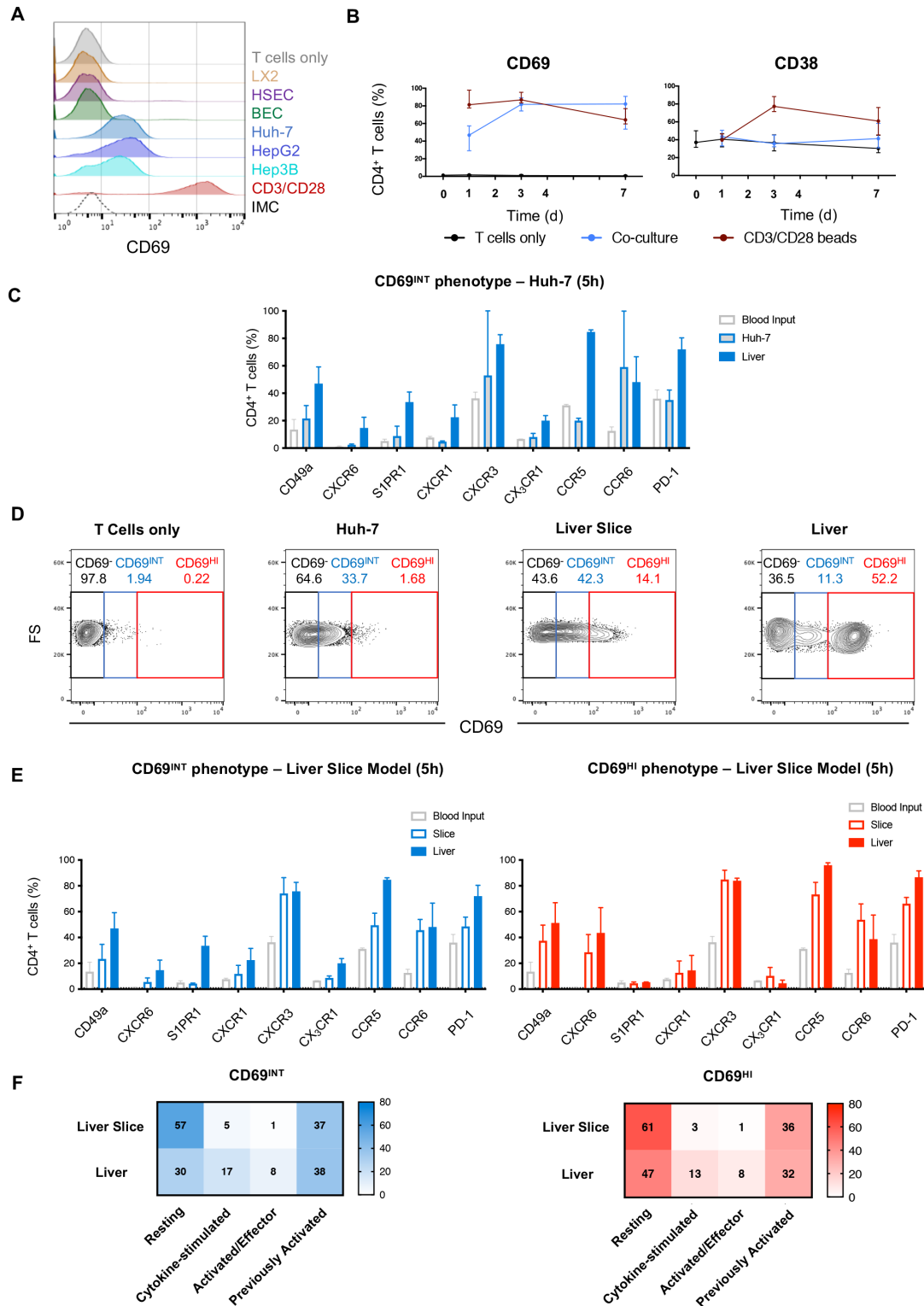


Figure 6 CD69^{INT}CD4⁺ and CD69^{HI} CD4⁺ T cells are differentially induced by the liver microenvironment. (A) % CD69 expression on PBMC-derived CD4⁺ T cells cultured for 16 hours with primary HSEC, primary BEC; hepatic stellate cell line LX-2; hepatocyte cell lines HuH-7, HepG2 or Hep3B; with anti-CD3/CD28; or alone. Histogram displays representative CD69 expression levels in each condition. (B) % CD69 and CD38 expressions on blood CD4⁺ T cells over a 7-day culture period with HuH-7 (n=8–10/timepoint). (C) Comparison of key phenotypical markers in Huh-7-generated CD69^{INT} cells from PBMC following 5-hour culture, matched patient IHL CD69^{INT} cells and blood T cells alone (n=2). (D) Representative flow plots showing degree of CD69^{INT} and CD69^{HI} generation within PBMC after 5 hours of culture: alone, with Huh-7 cells, with precision-cut donor-matched liver slices; or from directly isolated IHLs from matched human liver. (E) Comparison of CD69^{INT} cells (left) and CD69^{HI} cells (right) generated from donor-matched PBMCs in a precision-cut liver slice model, with matched donor-derived liver populations, and input blood CD4⁺ T cells alone (n=2). (F) Activation/differentiation statuses of CD69^{INT} and CD69^{HI} cells in the different conditions as assessed by KLRG-1/CD127 costaining patterns (as in figure 3E). Colour intensity and displayed numbers represent median % in each KLRG-1/CD127 designation. BEC, biliary epithelial cell; FS, forward scatter; HL, intrahepatic lymphocyte; HSEC, hepatic sinusoidal endothelial cell; IMC, isotype-matched control.

supplemental figure 8C–D). *In vitro*-generated CD69^{INT}CD4⁺ T cells partially recapitulated the phenotypical signature of intrahepatic CD69^{INT}CD4⁺ T cells observed *ex vivo* after just 5 hours in culture, with upregulation of CXCR3 and CD49a, but not S1PR1, CXCR1 or CX₃CR1 (figure 6C). CD69^{INT}CD4⁺ T cells generated *in vitro* were also capable of producing IL-4 on stimulation, again resembling intrahepatic CD69^{INT}CD4⁺ T cells (online supplemental figures 4 and 9). Thus, short-term contact with hepatic epithelia can induce a population of CD69^{INT}CD4⁺ T cells *in vitro*.

We further considered whether additional signals from the liver microenvironment were required to generate CD69^{HI}CD4⁺ T cells. To investigate this, we used a coculture model of patient-derived PBMCs with autologous precision-cut liver slices to allow full retention of the native liver microenvironment (figure 6D). Coculture of autologous PBMC for 5 hours with matched liver slices led to an increase in T-cell expression of both intermediate and high levels of CD69, not seen with hepatic epithelia coculture. Remarkably, short-term slice-culture-generated CD69^{HI}CD4⁺ T cells phenotypically resembled *ex vivo* intrahepatic CD69^{HI}CD4⁺ T cells, with high expression of CXCR6, CD49a, CCR5 and PD-1, low expression of S1PR1 and a largely resting (KLRG-1⁻CD127⁺) phenotype (figure 6E–F). Correspondingly, CD69^{INT}CD4⁺ T cells also generated through hepatic slice culture acquired many of the phenotypical characteristics of their *ex vivo* counterparts, notably expression of CXCR3, and partial acquisition of the residency markers CD49a and CXCR6. Together these results suggest that CD4⁺ T cell contact with hepatic epithelia promotes their differentiation to a CD69^{INT}CD4⁺ phenotype in the liver, whereas the generation of CD69^{HI}CD4⁺ T_{RM} requires additional signals from the liver microenvironment.

DISCUSSION

In this study, we characterised two distinct CD69-expressing CD4⁺ T-cell populations in the human liver — a long-lived CD69^{HI}CD4⁺ T_{RM} subset, with a prototypical tissue-retention signature, a resting restrained phenotype and the ability to instigate type-1 multifunctional responses on stimulation; and a novel population of CD69^{INT}CD4⁺ T cells with a CXCR3⁺CXCR1⁺CX₃CR1⁺ phenotype that are more activated, recirculation-competent and skewed towards T_H2 responses on stimulation. We show that these two populations possess different generation requirements and are equipped to play differential roles in liver disease.

In agreement with other human CD4⁺ T_{RM} studies, liver CD69^{HI}CD4⁺ T cells expressed T_{RM}-associated retention molecules CD49a and CXCR6,^{8 16 39} have low expression of the homing receptors S1PR1 and CX₃CR1,¹³ a resting and restrained phenotype including high PD-1 expression,^{13 39} and the ability to produce T_H1 cytokines.^{33 34 39} CXCR6 is of particular importance as a key liver retention molecule that is required for residence of multiple lymphocyte subpopulations in the liver,^{40–42} and our data demonstrate that the liver microenvironment is able to rapidly induce a CXCR6⁺ signature in newly formed resident CD4⁺ T cells.

We recently described human liver CD8⁺ T_{RM} that share some of these key features (CXCR6⁺, PD-1⁺ and rapid functionality).⁵ Intriguingly, intrahepatic CD8⁺ T_{RM} in both mouse and humans are thought to uniquely reside within the liver vasculature.^{5 43 44} Our data suggest that liver CD69^{HI}CD4⁺ T_{RM} can also be found throughout the parenchyma, including within sinusoids. Candidate molecules for maintaining the

CD69^{HI}T_{RM} in this niche include CXCR6 through interactions with its ligand CXCL16, expressed on the sinusoidal lumen,^{23 40} or integrin αLβ2-ICAM interactions.⁴⁴ Furthermore, our findings suggest CD69^{HI}CD4⁺T_{RM} can be found in portal regions, likely directed specifically to portal vasculature by CCR5 ligands.⁴⁵ The strategic positioning of CD4⁺ T_{RM} in both vascular sites could allow efficient targeted immunosurveillance and opportunities to interact with other key immune cells within the liver. Finally, we demonstrated our CD69^{HI}CD4⁺T_{RM} are most likely enriched for IL-21⁺T_{FH}-like cells, in keeping with the emerging overlap between T_{FH} and T_{RM} phenotypes.^{46 47}

Hepatic CD69^{INT}CD4⁺ T cells have not been previously described. Functionally, CD69^{INT}CD4⁺ T cells were most able to produce the T_H2 cytokine IL-4. Key distinguishing features of hepatic CD69^{INT}CD4⁺ T cells were expression of CXCR3 and CXCR1 required for hepatocyte homing,²¹ and importantly, CX₃CR1. CD69^{INT}CD4⁺ T cells were also found in hLNs, consistent with a wide-ranging immune surveillance role, analogous to the CX₃CR1^{INT} ‘peripheral memory’ CD8⁺ T cells that survey peripheral tissues in both humans and mice.^{19 20} Further, a small population of non-resident CD69^{INT}CD8⁺ T cells in mice has been previously reported.⁴⁸ The ‘migratory memory’ CD4⁺ T cells described by Watanabe *et al* showed variable CD69 positivity and recirculated through the skin slower than conventional T_{CM}.⁴⁹ Interestingly, activated, recirculating CD69^{INT}CD4⁺ T cells, rather than resident CD69^{HI}CD4⁺ T cells correlated with necroinflammatory scores in CHB. This suggests CD69^{INT}CD4⁺ T-cell involvement in proinflammatory processes in chronic viral disease, but whether this contributes to the cause, or is a consequence of the inflammation, remains to be determined.

Although CD69^{INT}CD4⁺ T cells expressed a tissue egress signature (S1PR1 and CX₃CR1) and were found in the blood, these cells may also contain a population capable of long-term residence. While this resident pool could conceivably derive from resident CD69^{HI}CD4⁺ T cells, the clear disparity in chemokine receptor expression suggests this outcome is unlikely. Resident CD69^{HI}CD4⁺ T cells may use CXCR6 for long-term retention more than CD69^{INT}CD4⁺ T cells, allowing the possibility of distinct liver immunosurveillance roles. Alternatively, short-term resident populations may exist within the CD69^{INT}CD4⁺ pool, as has been described for murine tissue CD4⁺ T cells,⁵⁰ possibly with the potential to transdifferentiate into long-term ‘conventional’ CD69^{HI}T_{RM} or ‘alternative’ CD69^{INT}T_{RM}. Future studies using single-cell sequencing approaches or TCR-repertoire analysis to further dissect the CD69^{INT}CD4⁺ T-cell compartment are necessary to address these hypotheses.

Our data revealed insights into the mechanisms behind the generation of both CD69^{INT}CD4⁺ and CD69^{HI}CD4⁺ T cells. CD69^{INT}CD4⁺-like cells were generated following short-term direct contact with hepatic epithelial cell lines, and primary BEC. Although the molecular mechanism for this remains undefined, *in situ* hepatocyte contact may promote CD4⁺ T-cell CD69 upregulation to an intermediate level, increasing liver dwell time and allowing more efficient immunosurveillance. Conversely, CD69^{HI}CD4⁺ T cells required additional signals from the liver microenvironment, given that cells with this phenotype could only be formed from blood-derived CD4⁺ T cells when cocultured with autologous liver slices. Interestingly, robust initiation of a residency transcriptional programme can happen within 2 days in mice.⁴⁸ Cytokines such as IL-15 and TGF-β can induce a CD8⁺ T-cell tissue

residency programme,¹¹ and we previously demonstrated that combinations of both cytokines were sufficient to generate cells with a CD8⁺ T_{RM} phenotype.⁵ This raises the possibility that these cytokines provide the same additional signals for CD69^{HI}CD4⁺T_{RM} formation. Unfortunately, extension of liver-slice coculture beyond 5 hours was not technically possible. Mouse models could be used to better test the longevity of these phenotypes.

In conclusion, this study provides a phenotypical and functional framework for understanding liver CD4⁺ T_{RM} biology and characterises a novel heterogeneous CD69^{INT}CD4⁺ T-cell population that is shaped by the liver microenvironment. We suggest that for at least some peripheral tissues, binary expression of CD69 alone is not sufficient to define tissue-resident CD4⁺ T cells. This work will facilitate the understanding of the role of liver CD4⁺ T cells in hepatic immune homeostasis, with implications for the development of novel immunotherapeutic strategies for chronic liver diseases.

Author affiliations

¹Institute of Immunology and Immunotherapy, University of Birmingham, Birmingham, UK

²Institute of Immunity and Transplantation, Division of Infection and Immunity, University College London, London, UK

³Centre for Liver and Gastrointestinal Research, University of Birmingham, Birmingham, UK

⁴Department of Infectious Diseases and Guangdong Provincial Key Laboratory of Liver Disease Research, Third Affiliated Hospital of Sun Yat-Sen University, Guangzhou, China

⁵Immunobiology, Blizard Institute, London, UK

⁶Surgery, Royal Free Campus, UCL Medical School, London, UK

⁷Tissue Access for Patient Benefit, University College London, London, UK

⁸Department of Cellular Pathology, Royal Free Hospital, London, UK

⁹Centre for Liver Research, National Institute for Health Research Biomedical Research Unit, University of Birmingham, Birmingham, UK

¹⁰Department of Infectious Diseases, Third Affiliated Hospital of Sun Yat-sen University, Guangzhou, Guangdong, China

¹¹Guangdong Provincial Key Laboratory of Liver Disease Research, Third Affiliated Hospital of Sun Yat-sen University, Guangzhou, Guangdong, China

¹²Division of Infection and Immunity, Rayne Institute, University College London, London, UK

Twitter Benjamin G Wiggins @BenWiggins_093, Laura J Pallett @pallett_lab, Upkar S Gill @druppygill, Arzoo M Patel @arzi_x, Mala K Maini @maini_lab and Zania Stamataki @zaniastamataki

Acknowledgements We are grateful to all patients and donors at the Queen Elizabeth Hospital Birmingham, and the Royal Free Hospital, London. We thank the whole liver transplantation unit and all the clinical pathology team at the Queen Elizabeth Hospital for sample allocation; and all clinical staff who helped with patient recruitment across both centres including the Tissue Access for Patient Benefit project at The Royal Free Hospital. Thanks to Anthony Bolan (National Health Service, London, UK), and staff at the MRC Weatherall Institute of Molecular Medicine Sequencing Facility (Oxford, UK) for their help with HLA-haplotyping. Our thanks also to Loraine Brown and Bridget Gunson for their help with access and management of patient information and to the support staff at the UCL Infection and Immunity Flow Cytometry Core Facility.

Contributors BGW, LJP, MKM and ZS conceived the project, designed experiments, critically evaluated the data and edited the manuscript; BGW, LJP, XL, SPD, OEA, USG, AMP, SK, KA, YSL and GMR generated data; BGW, LJP, XL and SPD analysed data; USG, GMR, GH and PTFK provided access to patient material; BGW wrote the manuscript and carried out statistical comparisons; BGW, LJP, SPD and ZS constructed figures; YH, MKM and ZS acquired funding and supervised the project; all authors reviewed the manuscript. BGW, LJP and XL are joint first authors. YH, MKM and ZS are joint last authors.

Funding BGW and SPD were funded by PhD studentships from the Medical Research Council Centre for Immune Regulation, University of Birmingham. SPD was funded by an NC3R training fellowship. MKM and LJP are supported by Wellcome Trust Investigator award 214191/Z/18/Z and CRUK Immunology grant 26603. XL was funded by a Guangzhou Municipal Government (GMG 2016201604030021) award to YH and ZS. KA is funded by a Dr Falk studentship to GH. YSL was funded by an MRC Confidence in Concept Award to ZS. ZS was funded by the MRC, Wellcome Trust, GMG, The Birmingham Children's Hospital Research Foundation

the Royal Society and an intermediate career fellowship from the Medical Research Foundation. USG was funded by A Wellcome Trust Clinical Research Training Fellowship (107389/Z/15/Z), NIHR Academic Clinical Lectureship (018/064/A), Academy of Medical Sciences Starter Grant (SGL021/1030) and Seedcorn funding from Rosetrees/Stoneygate Trust (A2903). PTFK is supported by Barts Charity Project Grants (723/1795 and MGU/0406) and an NIHR Research for patient benefit award (PB-PG-0614-34087).

Competing interests BW collaborated with and received funding from Bioniz. LJP sat on advisory boards/provided consultancy for Gilead Sciences and SQZ Biotech. KA was funded by a studentship with Dr Falk. MKM received research funding from Gilead Sciences, Hoffmann La Roche and Immunocore. MKM sat on advisory boards/provided consultancy for Gilead, Hoffmann La Roche, Immunocore, VIR, Galapagos NV, GSK, Abbvie and Freeline. ZS collaborated with Bioniz and AstraZeneca and consulted for Boehringer Ingelheim. All other authors declare no conflict of interest.

Patient consent for publication Not required.

Ethics approval This study was approved by local research ethics committees in Birmingham and London. All samples were obtained with written informed patient consent. All study protocols complied with the 1975 Declaration of Helsinki.

Provenance and peer review Not commissioned; externally peer reviewed.

Data availability statement Data are available upon reasonable request.

Supplemental material This content has been supplied by the author(s). It has not been vetted by BMJ Publishing Group Limited (BMJ) and may not have been peer-reviewed. Any opinions or recommendations discussed are solely those of the author(s) and are not endorsed by BMJ. BMJ disclaims all liability and responsibility arising from any reliance placed on the content. Where the content includes any translated material, BMJ does not warrant the accuracy and reliability of the translations (including but not limited to local regulations, clinical guidelines, terminology, drug names and drug dosages), and is not responsible for any error and/or omissions arising from translation and adaptation or otherwise.

Open access This is an open access article distributed in accordance with the Creative Commons Attribution 4.0 Unported (CC BY 4.0) license, which permits others to copy, redistribute, remix, transform and build upon this work for any purpose, provided the original work is properly cited, a link to the licence is given, and indication of whether changes were made. See: <https://creativecommons.org/licenses/by/4.0/>.

ORCID iDs

Benjamin G Wiggins <http://orcid.org/0000-0001-5215-2004>

Laura J Pallett <http://orcid.org/0000-0002-4161-9462>

Patrick T F Kennedy <http://orcid.org/0000-0001-9201-0094>

Zania Stamataki <http://orcid.org/0000-0003-3823-4497>

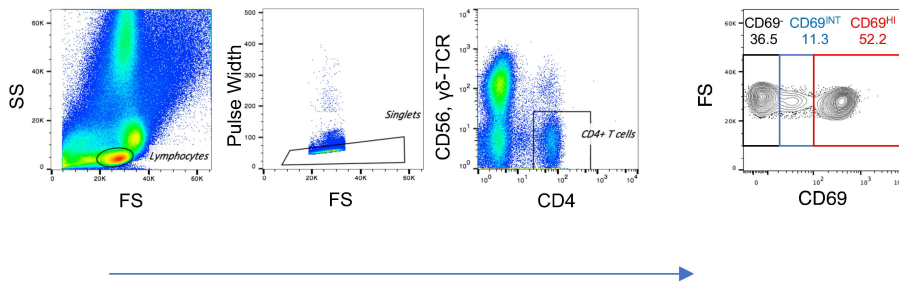
REFERENCES

- Clark RA. Resident memory T cells in human health and disease. *Sci Transl Med* 2015;7:269rv1.
- Schenkel JM, Fraser KA, Vezy V, et al. Sensing and alarm function of resident memory CD8⁺ T cells. *Nat Immunol* 2013;14:509–13.
- Beura LK, Fares-Frederickson NJ, Steinert EM, et al. CD4⁺ resident memory T cells dominate immunosurveillance and orchestrate local recall responses. *J Exp Med* 2019;216:1214–29.
- Park CO, Kupper TS. The emerging role of resident memory T cells in protective immunity and inflammatory disease. *Nat Med* 2015;21:688–97.
- Pallett LJ, Davies J, Colbeck EJ, et al. IL-2^{high} tissue-resident T cells in the human liver: Sentinels for hepatotropic infection. *J Exp Med* 2017;214:1567–80.
- Mueller SN, Mackay LK. Tissue-Resident memory T cells: local specialists in immune defence. *Nat Rev Immunol* 2016;16:79–89.
- Jiang X, Clark RA, Liu L, et al. Skin infection generates non-migratory memory CD8⁺ T(RM) cells providing global skin immunity. *Nature* 2012;483:227–31.
- Tejaro JR, Turner D, Pham Q, et al. Cutting edge: Tissue-retentive lung memory CD4 T cells mediate optimal protection to respiratory virus infection. *J Immunol* 2011;187:5510–4.
- Pan Y, Tian T, Park CO, et al. Survival of tissue-resident memory T cells requires exogenous lipid uptake and metabolism. *Nature* 2017;543:252–6.
- Pallett LJ, Schmidt N, Schurich A. T cell metabolism in chronic viral infection. *Clin Exp Immunol* 2019;197:143–52.
- Mackay LK, Wynne-Jones E, Freestone D, et al. T-Box transcription factors combine with the cytokines TGF- β and IL-15 to control tissue-resident memory T cell fate. *Immunity* 2015;43:1101–11.
- McMaster SR, Wilson JJ, Wang H, et al. Airway-Resident memory CD8 T cells provide antigen-specific protection against respiratory virus challenge through rapid IFN- γ production. *J Immunol* 2015;195:203–9.
- Kumar BV, Ma W, Miron M, et al. Human tissue-resident memory T cells are defined by core transcriptional and functional signatures in lymphoid and mucosal sites. *Cell Rep* 2017;20:2921–34.

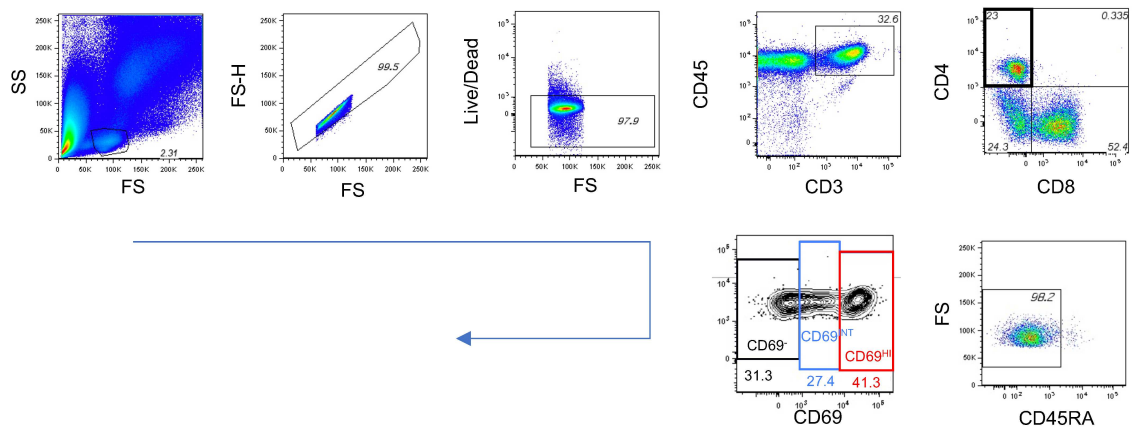
- 14 Turner DL, Farber DL. Mucosal resident memory CD4 T cells in protection and immunopathology. *Front Immunol* 2014;5:331.
- 15 Szabo PA, Miron M, Farber DL. Location, location, location: tissue resident memory T cells in mice and humans. *Sci Immunol* 2019;4. doi:10.1126/sciimmunol.aas9673. [Epub ahead of print: 05 04 2019].
- 16 Wong MT, Ong DEH, Lim FSH, et al. A high-dimensional atlas of human T cell diversity reveals tissue-specific trafficking and cytokine signatures. *Immunity* 2016;45:442–56.
- 17 Morland CM, Fear J, McNab G, et al. Promotion of leukocyte transendothelial cell migration by chemokines derived from human biliary epithelial cells in vitro. *Proc Assoc Am Physicians* 1997;109:372–82.
- 18 Lalor PF, Adams DH. The liver: a model of organ-specific lymphocyte recruitment. *Expert Rev Mol Med* 2002;4:1–15.
- 19 Gerlach C, Moseman EA, Loughhead SM, et al. The Chemokine Receptor CX3CR1 Defines Three Antigen-Experienced CD8 T Cell Subsets with Distinct Roles in Immune Surveillance and Homeostasis. *Immunity* 2016;45:1270–84.
- 20 Gordon CL, Lee LN, Swadlow L, et al. Induction and Maintenance of CX3CR1-Intermediate Peripheral Memory CD8⁺ T Cells by Persistent Viruses and Vaccines. *Cell Rep* 2018;23:768–82.
- 21 Adams DH, Ju C, Ramaiah SK. Mechanisms of immune-mediated liver injury. *Toxicological* 2010.
- 22 Gill US, Pallett LJ, Thomas N, et al. Fine needle aspirates comprehensively sample intrahepatic immunity. *Gut* 2019;68:1493–503.
- 23 Heydtmann M, Lalor PF, Eksteen JA, et al. Cxc chemokine ligand 16 promotes integrin-mediated adhesion of liver-infiltrating lymphocytes to cholangiocytes and hepatocytes within the inflamed human liver. *J Immunol* 2005;174:1055–62.
- 24 Pallett LJ, Burton AR, Amin OE, et al. Longevity and replenishment of human liver-resident memory T cells and mononuclear phagocytes. *J Exp Med* 2020;217. doi:10.1084/jem.20200050. [Epub ahead of print: 07 09 2020].
- 25 Testi R, D'Ambrosio D, De Maria R, et al. The CD69 receptor: a multipurpose cell-surface trigger for hematopoietic cells. *Immunol Today* 1994;15:479–83.
- 26 Agata Y, Kawasaki A, Nishimura H, et al. Expression of the PD-1 antigen on the surface of stimulated mouse T and B lymphocytes. *Int Immunol* 1996;8:765–72.
- 27 Henson SM, Akbar AN. KLRG1--more than a marker for T cell senescence. *Age* 2009;31:285–91.
- 28 Huang H-Y, Luther SA. Expression and function of interleukin-7 in secondary and tertiary lymphoid organs. *Semin Immunol* 2012;24:175–89.
- 29 Thome JJC, Yudanin N, Ohmura Y, et al. Spatial map of human T cell compartmentalization and maintenance over decades of life. *Cell* 2014;159:814–28.
- 30 Kannanganat S, Ibegbu C, Chennareddi L, et al. Multiple-cytokine-producing antiviral CD4 T cells are functionally superior to single-cytokine-producing cells. *J Virol* 2007;81:8468–76.
- 31 Seder RA, Darrah PA, Roederer M. T-Cell quality in memory and protection: implications for vaccine design. *Nat Rev Immunol* 2008;8:247–58.
- 32 Sathaliyawala T, Kubota M, Yudanin N, et al. Distribution and compartmentalization of human circulating and tissue-resident memory T cell subsets. *Immunity* 2013;38:187–97.
- 33 Purwar R, Campbell J, Murphy G, et al. Resident memory T cells (T(RM)) are abundant in human lung: diversity, function, and antigen specificity. *PLoS One* 2011;6:e16245.
- 34 Booth JS, Toapanta FR, Salerno-Goncalves R, et al. Characterization and functional properties of gastric tissue-resident memory T cells from children, adults, and the elderly. *Front Immunol* 2014;5:294.
- 35 Singal AK, Kamath PS. Model for end-stage liver disease. *J Clin Exp Hepatol* 2013;3:50–60.
- 36 Suk-Fong Lok A. Hepatitis B treatment: what we know now and what remains to be Researched. *Hepatal Commun* 2019;3:8–19.
- 37 Goodman ZD. Grading and staging systems for inflammation and fibrosis in chronic liver diseases. *J Hepatol* 2007;47:598–607.
- 38 Maini MK, Boni C, Lee CK, et al. The role of virus-specific CD8(+) cells in liver damage and viral control during persistent hepatitis B virus infection. *J Exp Med* 2000;191:1269–80.
- 39 Oja AE, Piet B, Helbig C, et al. Trigger-happy resident memory CD4⁺ T cells inhabit the human lungs. *Mucosal Immunol* 2018;11:654–67.
- 40 Geissmann F, Cameron TO, Sidobre S, et al. Intravascular immune surveillance by CXCR6⁺ NKT cells patrolling liver sinusoids. *PLoS Biol* 2005;3:e113.
- 41 Stegmann KA, Robertson F, Hansi N, et al. Cxcr6 marks a novel subset of T-betloEomeshi natural killer cells residing in human liver. *Sci Rep* 2016;6:26157.
- 42 Tse S-W, Radtke AJ, Espinosa DA, et al. The chemokine receptor CXCR6 is required for the maintenance of liver memory CD8⁺ T cells specific for infectious pathogens. *J Infect Dis* 2014;210:1508–16.
- 43 Fernandez-Ruiz D, Ng WY, Holz LE, et al. Liver-Resident Memory CD8⁺ T Cells Form a Front-Line Defense against Malaria Liver-Stage Infection. *Immunity* 2016;45:889–902.
- 44 McNamara HA, Cai Y, Wagle MV, et al. Up-Regulation of LFA-1 allows liver-resident memory T cells to patrol and remain in the hepatic sinusoids. *Sci Immunol* 2017;2. doi:10.1126/sciimmunol.aaj1996. [Epub ahead of print: 17 03 2017].
- 45 Oo YH, Shetty S, Adams DH. The role of chemokines in the recruitment of lymphocytes to the liver. *Dig Dis* 2010;28:31–44.
- 46 Künzli M, Schreiner D, Pereboom TC, et al. Long-Lived T follicular helper cells retain plasticity and help sustain humoral immunity. *Sci Immunol* 2020;5. doi:10.1126/sciimmunol.aay5552. [Epub ahead of print: 06 03 2020].
- 47 Chen M-M, Xiao X, Lao X-M, et al. Polarization of tissue-resident TFH-Like cells in human hepatoma bridges innate monocyte inflammation and M2b macrophage polarization. *Cancer Discov* 2016;6:1182–95.
- 48 Skon CN, Lee J-Y, Anderson KG, et al. Transcriptional downregulation of S1PR1 is required for the establishment of resident memory CD8⁺ T cells. *Nat Immunol* 2013;14:1285–93.
- 49 Watanabe R, Gehad A, Yang C, et al. Human skin is protected by four functionally and phenotypically discrete populations of resident and recirculating memory T cells. *Sci Transl Med* 2015;7:279ra39.
- 50 Collins N, Jiang X, Zaid A, et al. Skin CD4(+) memory T cells exhibit combined cluster-mediated retention and equilibration with the circulation. *Nat Commun* 2016;7:11514.

Supplementary Figure 1 – Gating strategies used to identify and compare hepatic CD69⁺, CD69^{INT} and CD69^{HI} cells.

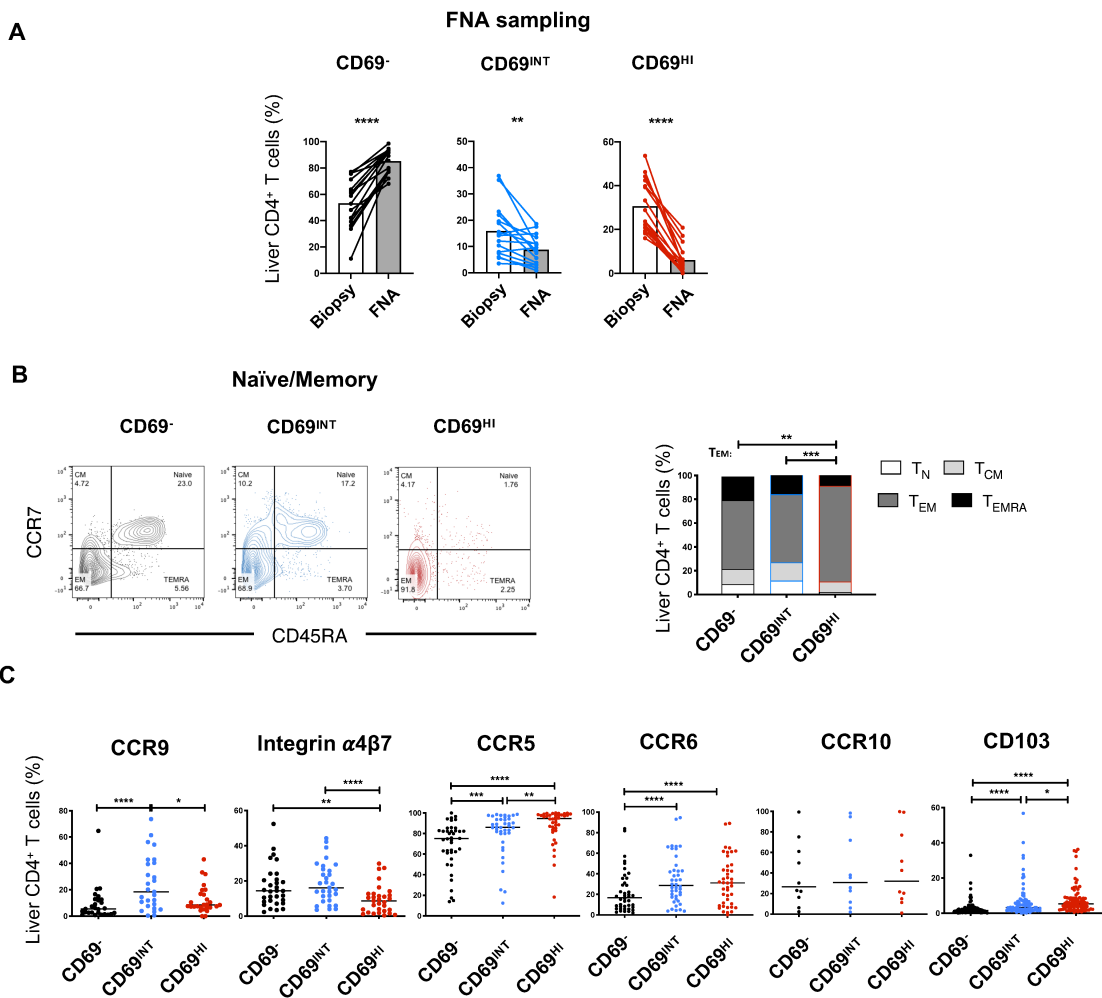
A

Centre A

B

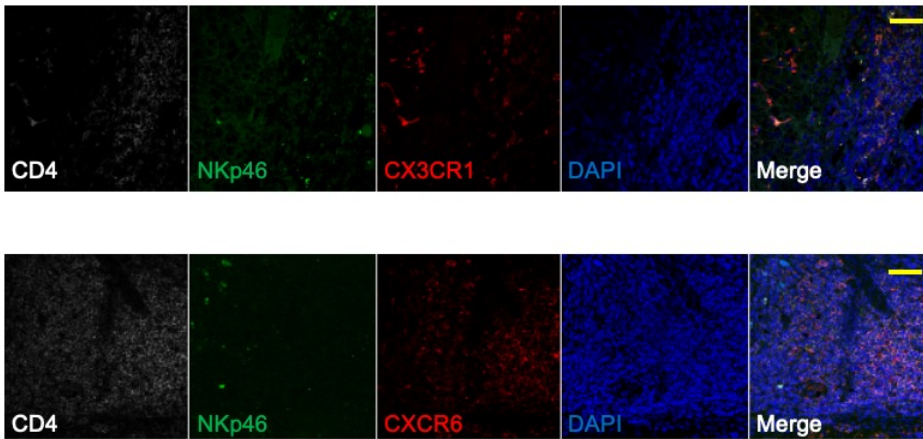
Centre B

Supplementary Figure 2 – Homing, location, and naïve/memory profiles of CD69-delimited subsets.

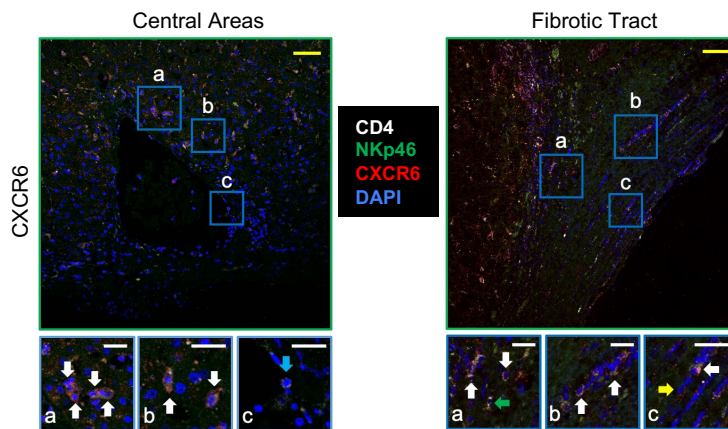


Supplementary Figure 3 - Localisation of CXCR6- and CX₃CR1-expressing CD4⁺T-cells throughout the liver

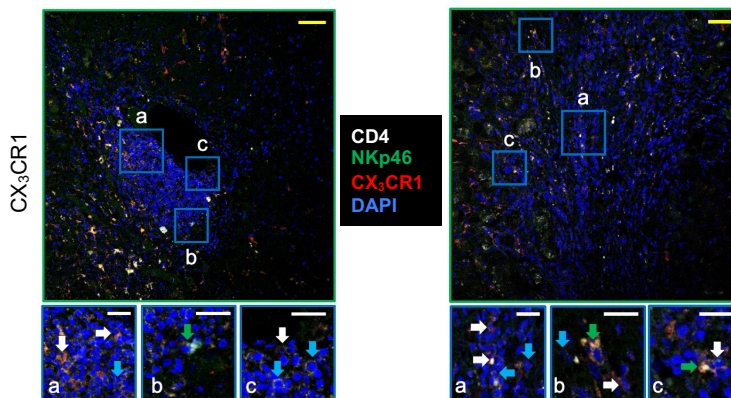
A



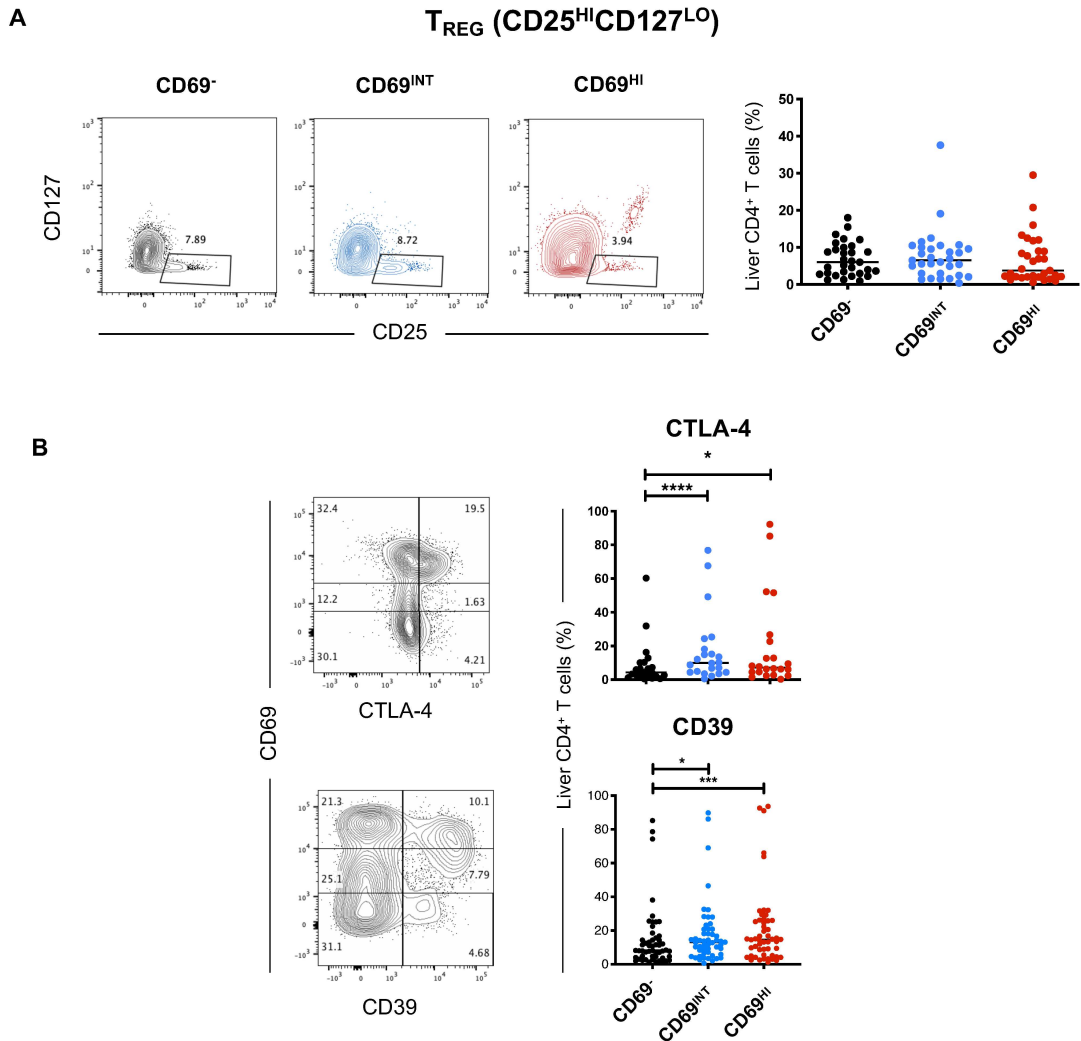
B



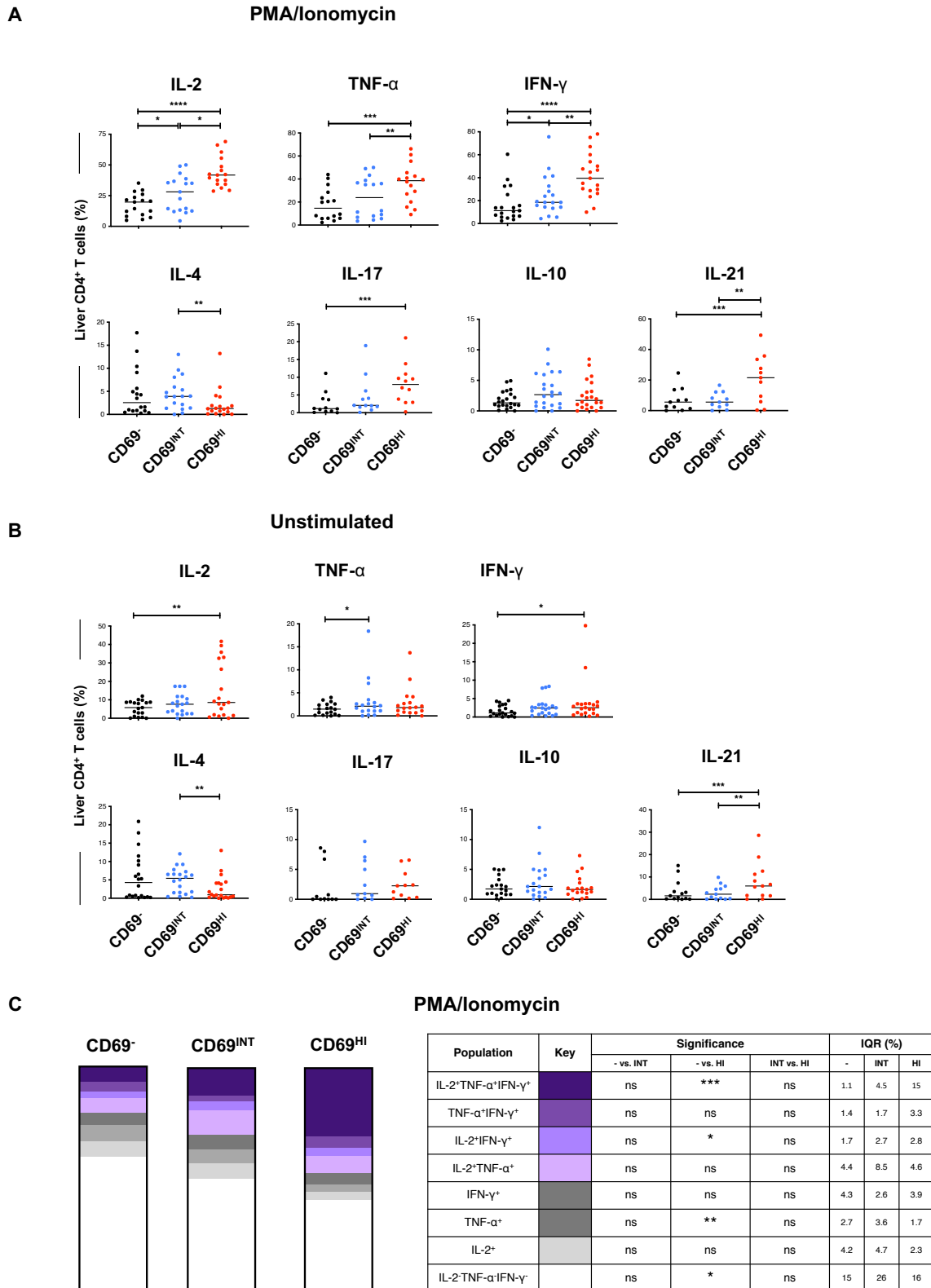
C



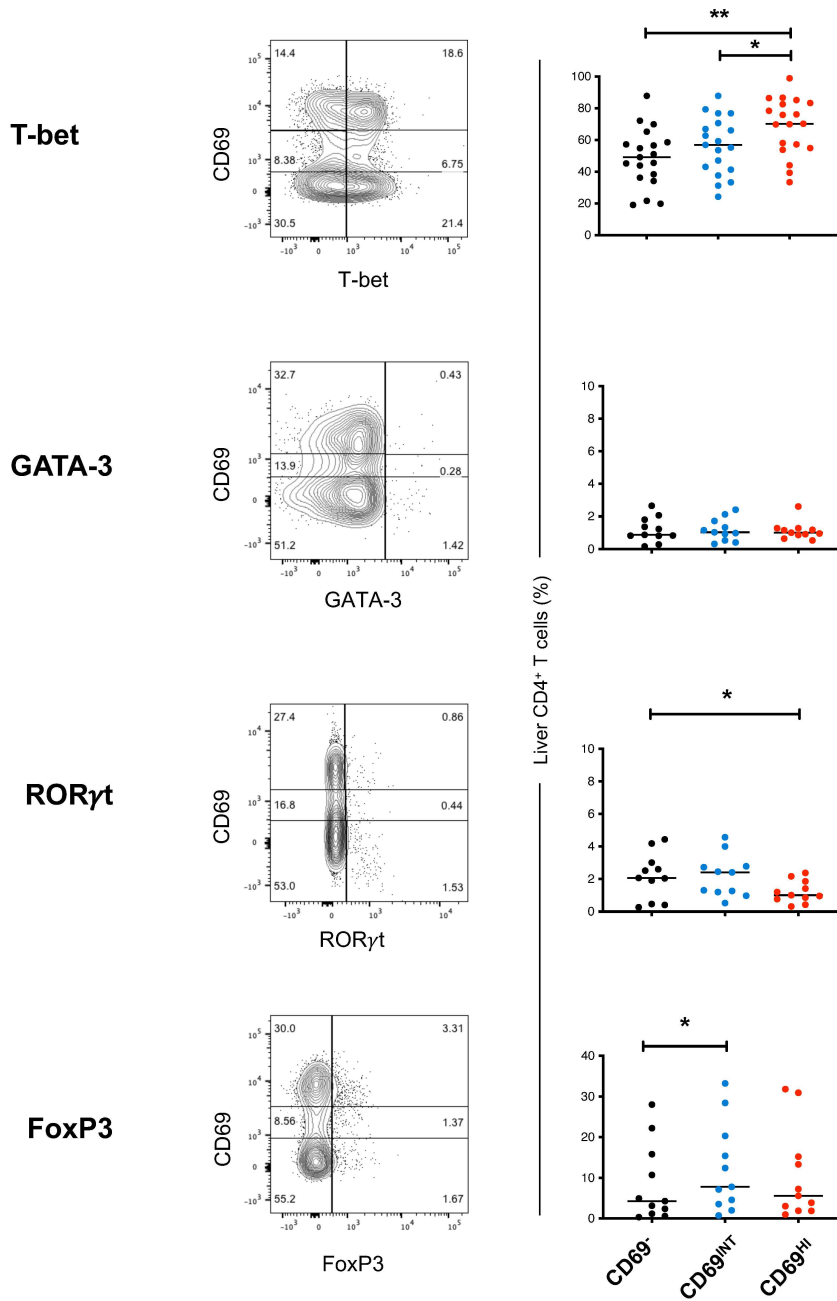
Supplementary Figure 4 – Conventional regulatory T cells are not enriched in any CD69-designated subset.



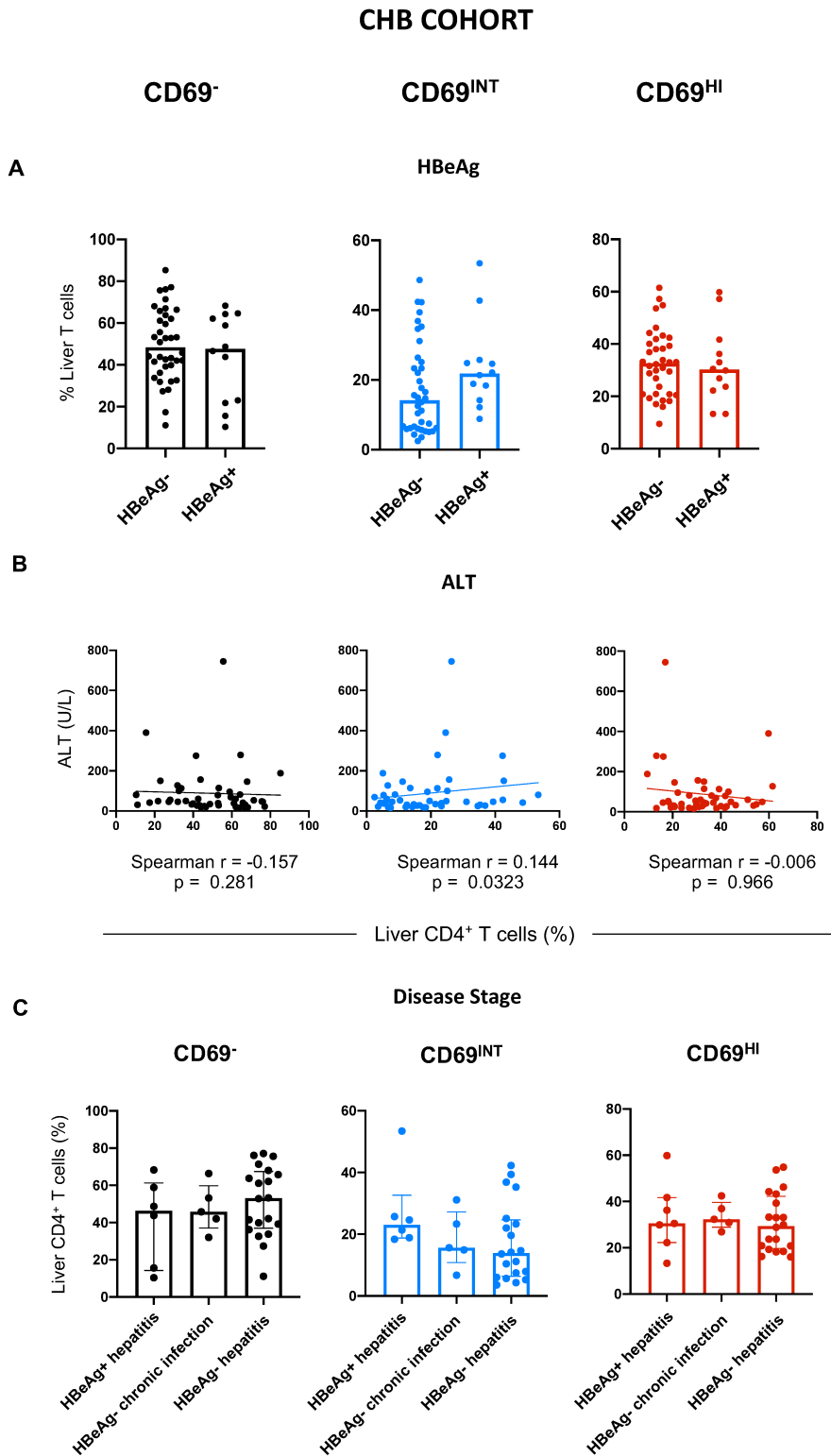
Supplementary Figure 5 – Differential cytokine responses of intrahepatic subsets marked by CD69 expression.



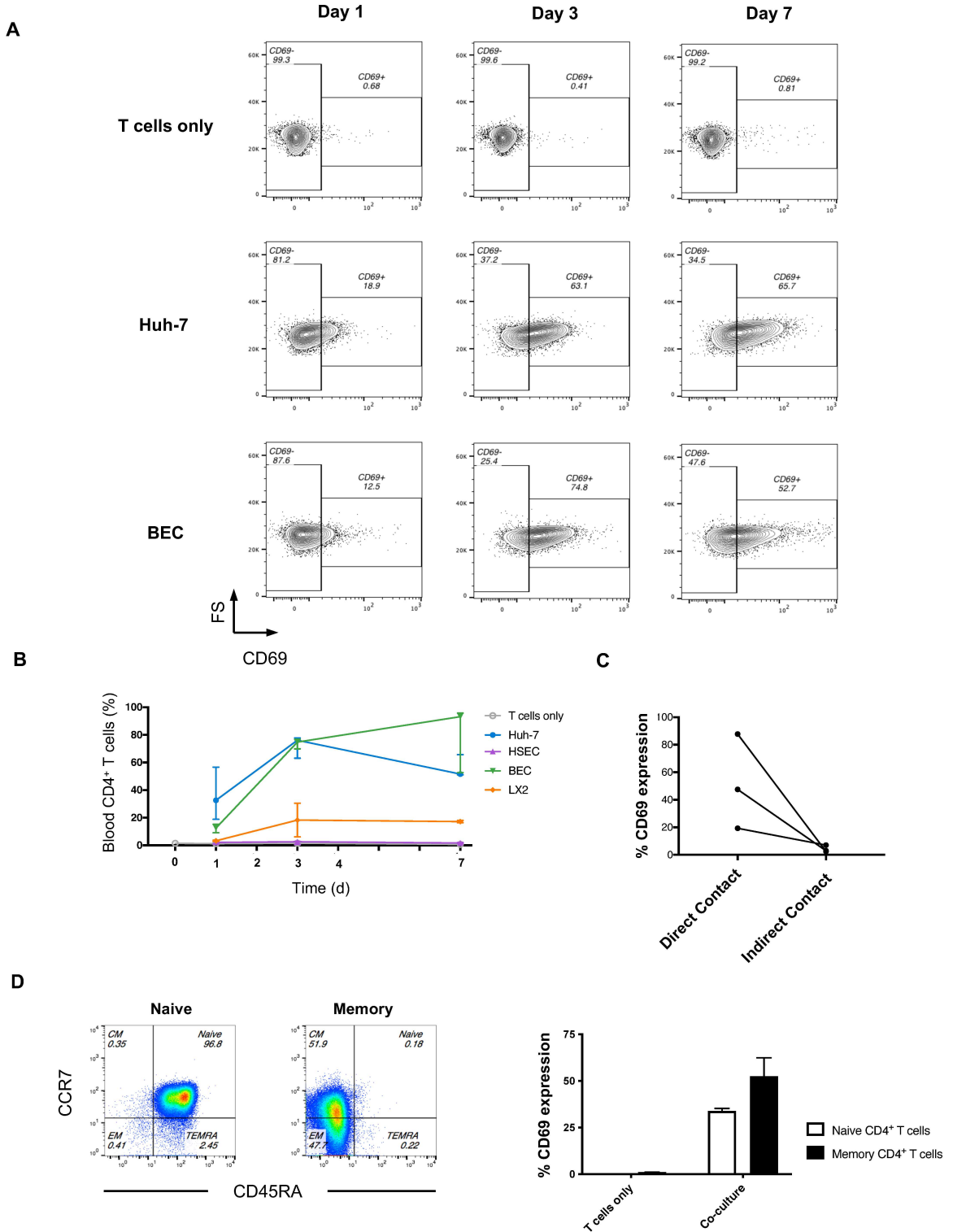
Supplementary Figure 6 – Transcription Factor profiles of Liver CD4⁺ T cell subsets



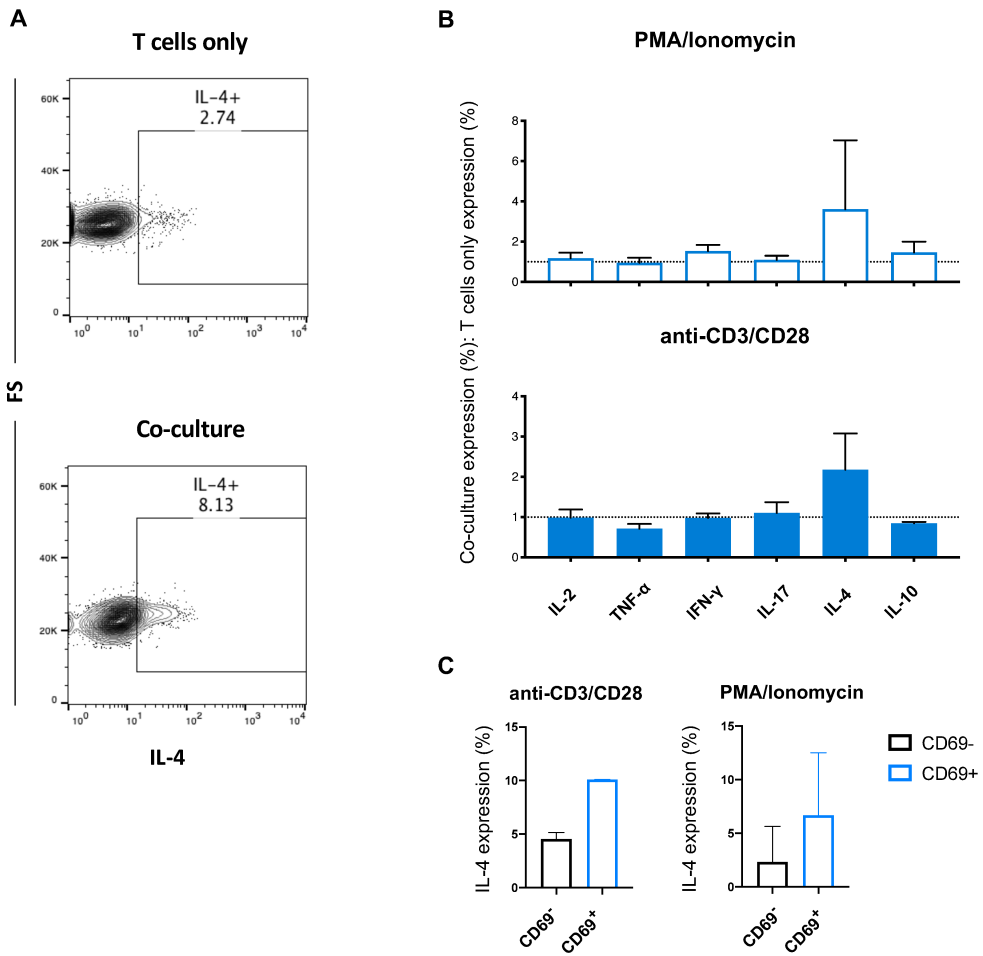
Supplementary Figure 7 – Additional correlation analysis with clinical parameters in HBV patient livers.



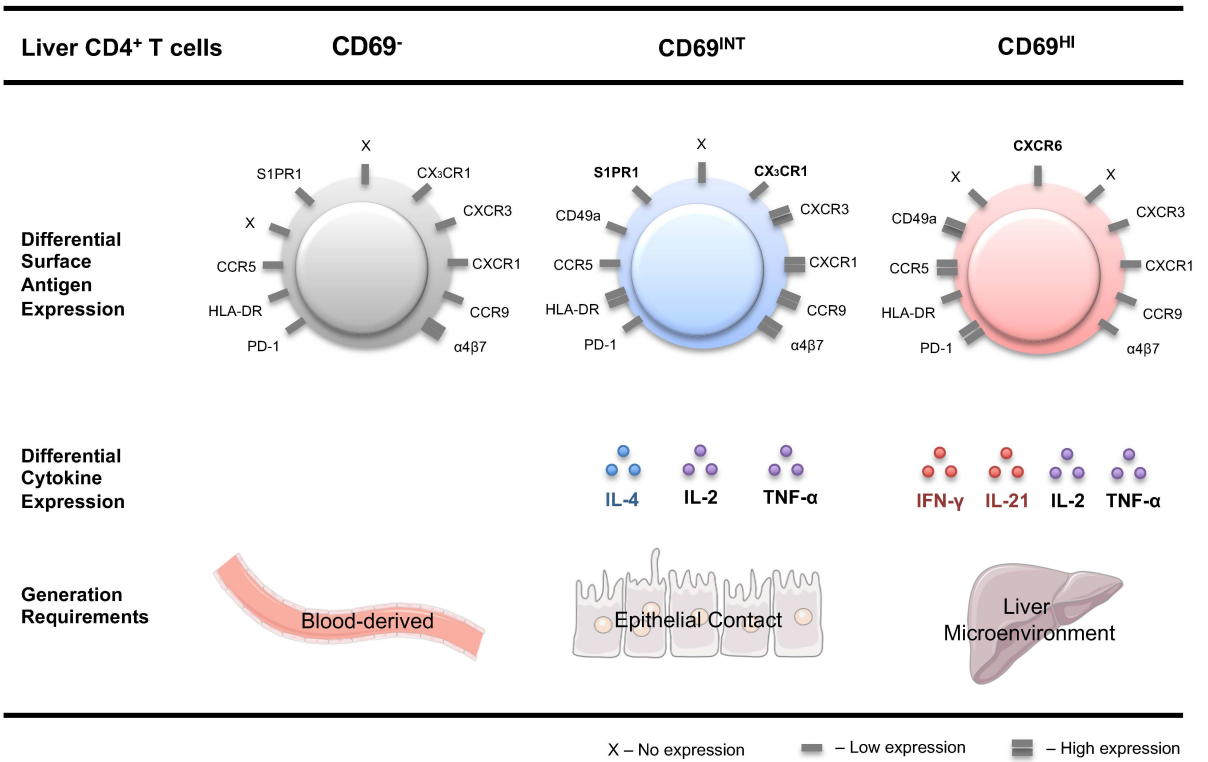
Supplementary Figure 8 – CD69^{INT} generation occurs with primary human epithelia, is contact-dependent, and more efficient in memory T cells



Supplementary Figure 9 – Co-culture with hepatic epithelia infers CD4⁺ T cells with IL-4 production capacity.



Graphical Abstract:



The liver shapes CD4⁺ T cells**Supplementary information:****Supplementary Experimental Procedures****Immune cell isolation**

Peripheral blood mononuclear cells (PBMCs) were isolated from human blood by density centrifugation (Lympholyte-H [Cederlane] – centre A, Ficoll-Hypaque plus [GEHealthcare] – centre B). Intrahepatic lymphocytes (IHL) were isolated through either chopping, multiple PBS washes, digestion with a stomacher machine (Seward), filtering out debris and density centrifugation (centre A); or for centre B biopsies – mechanical disruption with cell scrapers, filtration to remove debris, centrifugation. Larger centre B resections and explants: enzymatic digestion (30min incubation at 37°C with 0.02% Collagenase IV [Thermo-Fisher] 0.002% DNase I [Sigma-Aldrich]), mechanical disruption through a GentleMACS dissociator (Miltenyi Biotec), then 70µm filtering and centrifugation as above. Lymph node and spleen mononuclear cells were isolated through manual dissection, GentleMACS dissociation, filtration, and density centrifugation on Lympholyte-H (centre A); or manual dissection, filtration, and centrifugation on a Pancoll (PanBiotec) gradient. Intraepithelial lymphocytes (IEL) were isolated from the duodenum and ileum of the gut by enzymatic digestion (1hr incubation at 37°C shaking [180rpm] with 0.15% Collagenase IV [Thermo-Fisher] 0.02% DNase I [Sigma-Aldrich] 0.0025% Hyaluronidase Type IV-S [Sigma-Aldrich] 0.00125% Liberase DL [Roche]), mechanical disruption using a syringe, then 70µm filtration and centrifugation on a Pancoll gradient as above. The isolation of IHLs from FNA samples was undertaken as previously described³⁵. In brief, samples were centrifuged; the remaining cell pellet was re-suspended in 2mL of red blood cell lysis buffer (Biolegend) for 5min on ice, prior to staining. All samples were used immediately. Any samples for later use were frozen in 10% DMSO (Sigma-Aldrich) in fetal bovine serum (FBS) and stored in accordance with the Human Tissue Act.

Antibodies for Immunofluorescence

The following antibodies were used: mouse anti-human CD4 (Novus Biologicals; NBP2-46149), mouse anti-human NKp46 (R&D systems, UK; MAB1850), Rabbit anti-human CX3CR1 (ThermoFisher, UK; 702321) and rabbit-human CXCR6 (Abcam, UK; ab8023). Single stains and IMCs were used to ensure specificity. Secondary antibodies were all purchased from Thermo-Fisher Scientific.

T cell culture for stimulation experiments

PBMCs/IHLs were pre-stained with antibodies against CD69, CD4, CD56, and $\gamma\delta$ -TCR (centre A only), washed twice in PBS, and plated out in 96-well plates at 10⁶ cells/well in T-cell media (RPMI [ThermoFisher] + 10% FBS (Sigma-Aldrich), 100U/ml penicillin, 100µg/ml streptomycin, 1% non-essential amino acids (NEAA), 1% L-glutamine [all ThermoFisher Scientific, UK]) containing T cell stimulants.

T cell co-culture experiments

Hepatic cell lines all cultured in 24-well plates in 1ml media as follows: Huh-7, HepG2, Hep3B – all in complete DMEM (ThermoFisher): DMEM + 10% FBS, 100U/ml penicillin,

The liver shapes CD4⁺ T cells

100µg/ml streptomycin, 1% NEAA, 1% L-glutamine; LX-2 – as above but 2% FBS; primary BEC – 1:1 Ham's F12 media (ThermoFisher) & DMEM + 10% heat activated human serum (HD supplies) 2mM Penicillin/Streptomycin, 10µg/L epidermal growth factor, 10µg/L hepatocyte growth factor (both Peptotech), 124 IU/L Insulin, 20µg/L Hydrocortisone (both QE hospital pharmacy, Birmingham), 10µg/L Cholera Toxin, 0.2nM Tri-iodothyronine (both Sigma-Aldrich); primary HSEC – Human Endothelial Serum free media (ThermoFisher) + 10% heat activated human serum, 10µg/L hepatocyte growth factor, 10µg/L vascular endothelial cell growth factor (Peptotech). BEC and HSEC cultured on type-1 rat-tail collagen (Sigma Aldrich, UK) coated plates (coated with 40µg/ml solution). Once adhered to plate, T cells added to 1ml wells in 100µl of T-cell media.

Supplementary Figures:

Supplementary Figure 1 – Gating strategies used to identify and compare hepatic CD69⁻, CD69^{INT} and CD69^{HI} cells. Gating strategy used in centre A (**A**), and B (**B**) where blue arrows represent direction of gating (onward gate in bold when multiple in one plot).

Supplementary Figure 2 – Homing, location, and naïve/memory profiles of CD69-delimited subsets. **A** – Comparison of each subset (%) recovered from liver tissue digests or fine needle aspirate (FNA) samples. **B** – proportion of liver CD4⁺ T cells in each subset that comprise naïve, central memory (T_{CM}), effector memory (T_{EM}), or T_{EMRA} as shown in representative plots and combined stack chart (n=51). **C** – Expression of additional homing/retention molecules in each subset. **D** – Immunofluorescent staining of formaldehyde-fixed paraffin-embedded liver sections (from patient with PBC). White arrows indicate CX₃CR1⁺ CD4⁺ T cells. Statistical comparisons by Wilcoxon matched-pairs signed rank tests (part A); Freidman tests with Dunn's multiple tests for parts B-C.

Supplementary Figure 3 - Localisation of CXCR6- and CX₃CR1-expressing CD4⁺T-cells throughout the liver. **A** – Example stains for each chemokine receptor merged and split by channel. **B** – Presence of cells of interest in central areas (**D**), and fibrotic areas (**E**). Central areas n=14 (5 donor, 4 HBV, 5 PBC), fibrotic areas n=9 (4 HBV, 5 PBC). Areas of interest a-c show higher magnification of cells of interest (white arrows – cell of interest, green arrows – NKp46⁺ cell, yellow arrow – chemokine receptor⁺ CD4⁺ cell. Yellow scale bars - 50µm, white scale bars – 20µm.

Supplementary Figure 4 – Conventional regulatory T cells are not enriched in any CD69-designated subset. **A** – Representative gating for T_{REGS} (CD25^{HI}CD127^{LO}) in each subset. Violin plot shows combined expression data. **B** – Expression of T_{REG} cardinal features in each subset – CTLA-4 and CD39 by representative staining and combined total data. Freidman tests with Dunn's multiple tests used for statistical comparison throughout.

Supplementary Figure 5 – Differential cytokine responses of intrahepatic subsets marked by CD69 expression. **A** – Cytokine expression following 5-hour stimulation of IHL with PMA and Ionomycin, followed by intracellular staining. IL-2 (n=17), TNF-α (n=16), IFN-γ (n=19), IL-4 (n=18), IL-17 (n=12), IL-10 (n=17), IL-21 (n=11). **B** – Expression of cytokines following 5hr in absence of stimulation, followed by intracellular staining. IL-2 (n=19), TNF-α (n=18), IFN-γ (n=21), IL-4 (n=20), IL-17 (n=11), IL-10 (n=19), IL-21 (n=13). **C** - Multi-functional responses of liver CD69⁻, CD69^{INT}, and CD69^{HI} CD4⁺ T cells following 5-hour PMA/Ionomycin stimulation. Stacked bar chart heights represent median % of each combination of IL-2/TNF-α/IFN-γ-expressing cells as shown (n=7). Table displays statistical significance between the

The liver shapes CD4⁺ T cells

three populations, and interquartile range values. Freidman tests with Dunn's multiple tests used to compare matched populations throughout.

Supplementary Figure 6 – Transcription Factor profiles of Liver CD4⁺ T cell subsets. Representative plots and combined % expression of T-bet (n=19), GATA-3, Ror γ t and FoxP3 (all n=11) amongst CD69-designated subsets. Freidman tests with Dunn's multiple tests used for statistical comparisons.

Supplementary Figure 7 – Additional correlation analysis with clinical parameters in HBV patient livers. A – Frequency of each subset in Hepatitis B e antigen positive vs – negative patients (Mann Whitney Test). **B** – Correlation of patient serum ALT against frequency of each subset. Spearman's correlation analysis p and r values given. **C** – Frequency of each subset in chronic HBV patient donor livers at each HBV disease stage. Disease staging of HBV donors determined by combination of HBeAg, HBV DNA, and serum ALT (compared by Kruskal-Wallis tests with multiple Dunn's post-hoc testing). Only 1 donor was at immunotolerant stage, so this stage excluded from dataset shown.

Supplementary Figure 8 – CD69^{INT} generation occurs with primary human epithelia and is contact-dependent. CD69 expression in peripheral blood-derived CD4⁺ T cells following co-culture for 1,3, and 7 days alone, with Huh-7 cells, or BEC. Data displayed as representative flow cytometry plots (**A**), and combined donor data alongside HSEC and LX-2 culture conditions (**B**). Median + 95% CI shown (n=3). **C** – CD69% expression amongst PBMC-derived CD4⁺ T cells when either cultured overnight with Huh-7 cells directly (direct contact), or when separated by a 0.4 μ m pore transwell insert (indirect contact). **D** – Naïve/Memory CD4⁺ T cell purity following isolation, followed by % CD69 expression following 16h co-culture with Huh-7 cells (n=1, 2 technical replicates).

Supplementary Figure 9 – Co-culture with hepatic epithelia infers CD4⁺ T cells with IL-4 production capacity. CD4⁺ T cells isolated from healthy human blood were cultured for 5 hours either alone or with Huh-7 hepatic epithelial cells, harvested and stimulated for 4 hours with anti-CD3/CD28 or PMA/Ionomycin, and then assessed for their ability to produce prototypic T cell cytokines by intracellular staining and flow cytometry. **A** – Staining example for IL-4 in T cells alone and following co-culture (PMA/Ionomycin stimulation). **B** – % expression of all the cytokines studied in co-cultured cells as a fold change from control (T cell only) cells (anti-CD3/CD28 – top, PMA/Ionomycin stimulation – bottom). **C** – Percentage expression of IL-4 in co-cultured CD69⁺ versus co-cultured CD69⁻ cells (both stimulation methods shown). Data from this experiment compiled from three independent donors.

The liver shapes CD4⁺ T cells

Supplementary Tables:

Supplementary Table 1 – Patient information for Liver tissue donors.

Shown are the disease breakdowns, sample type acquired and donor numbers in each group, together with median and IQR of the ages, and gender in each group. Numbers of donors acquired from each centre (A – University of Birmingham, B – University College London). AIH – Autoimmune hepatitis, ALD – Alcoholic liver disease, ARLD – Alcohol-related liver disease, BCM – breast cancer metastasis, CRC – colorectal cancer, HBV – hepatitis B virus, HCC – hepatocellular carcinoma, HCV – hepatitis C virus, MM – melanoma metastasis, NASH – non-alcoholic steatohepatitis, PBC – Primary biliary cholangitis, PSC – primary sclerosing cholangitis, NCPH – non-cirrhotic portal hypertension, SBC – secondary biliary cholangitis. * - 2 patient ages missing, ** - 3 patient ages missing, *** - 6 patient ages missing, † - 2 patient genders missing, †† - 4 patient genders missing, ††† - 6 patient genders missing from available data.

Aetiology	Sample Type	Numbers	Median age (IQR)	% Female	Centre A/B
Control	Donor Explant	12	51 (22)*	25 ^{††}	A(8) B(4)
Control	Pre-implant donor biopsy	7	39* (14)	33 ^{††}	B
Control	CRC margin	45	61 (18)***	20 ^{††}	B
Control	HCC margin	11	62.5 (8.8)**	25 [†]	B
Control	BCM margin	1	57	100	B
Control	MM margin	1	83	0	B
Control	PLD	3	61 (7)	100	A
HBV	Explant	4	39 (3)*	50 [†]	A(1) B(3)
HBV	Biopsy	51	35 (17.25)	29 ^{†††}	B
ALD	Explant	20	59 (14.3)	15	A
ARLD	Explant	1	48	0	B
NASH	Explant	8	60.5 (9.3)	50	A
NASH	Explant	1	51	0	B
PBC	Explant	7	44 (11.5)	71	A
PSC	Explant	12	35.5 (12.3)	25	A
AIH	Explant	1	21	0	A
HCV	Explant	2	59 (6)	0	A
HCV	Explant	3	61 (9)	33	B
Cryptogenic	Explant	2	53.5 (10.5)	50	A
Budd Chiari	Explant	1	31	0	A
NCPH	Explant	1	63	0	A
SBC	Explant	1	58	100	A

The liver shapes CD4⁺ T cells

Supplementary Table 2 – Patient information for lymph node, gut and spleen donors

Aetiology	Sample Type	Numbers	% Female	Centre A/B
Donor	Hepatic hilar LN	6	A(4) B(2)	
Donor	Non-hepatic LN (mesenteric)	6	B	
Donor	Biopsy – Duodenum	4	B	
Donor	Biopsy – Ileum	2	B	
Donor	Spleen	4	A(1) B(2)	

Supplementary Table 3 – Antibodies used in flow cytometry experiments

Antigen	Fluorochrome	Manufacturer	Clone	Catalogue Number
Phenotype				
CCR10	PE	Biolegend	6588-5	341504
CCR5	PE	Biolegend	J418F1	359106
CCR6	AlexaFluor488	Biolegend	G034E3	353414
CCR7	PE-Cy7	Biolegend	G043H7	353226
CCR9	PerCP-Cy5.5	Biolegend	L053E8	358906
CD103	APC	BD Biosciences	Ber-ACT8	563883
CD103	BV605	Biolegend	Ber-ACT8	350218
CD103	FITC	Biolegend	Ber-ACT8	350203
CD127	BV510	Biolegend	A019D5	351332
CD25	PE-Cy5	Biolegend	BC96	302608
CD27	FITC	Biolegend	M-T271	356404
CD3	BV711	Biolegend	OKT3	317328
CD3	BV711	BD Biosciences	UCHT1	563546
CD38	APC-Vio770	Mltenyi Biotec	REA572	130-099-151
CD39	BV421	Biolegend	A1	328214
CD4	APC	BD Biosciences	RPA-T4	555349
CD4	BV510	Biolegend	SK3	344634
CD4	FITC	Biolegend	OKT4	317408
CD4	APC-Cy7	BD Biosciences	RPA-T4	557871
CD4	BV421	BD Biosciences	RPA-T4	562425
CD45	BUV805	BD Biosciences	HI30	564914
CD45RA	BV421	BD Biosciences	HI100	562885
CD45RA	PE-Cy7	Biolegend	HI100	3014126
CD45RA	eFluor450	Thermo Fisher	HI100	48-0458-41
CD49a	PE	Biolegend	TS2/7	328304
CD49d	BV421	Biolegend	9F10	304322
CD56	APC-Vio770	Mltenyi Biotec	REA196	130-100-690
CD56	BUV395	BD Biosciences	NCAM16.2	563555
CD69	FITC	BD Biosciences	FN50	560969
CD69	PE-Dazzle594	Biolegend	FN50	310942
CD69	BV605	Biolegend	FN50	310937
CD8	BV786	Biolegend	RPA-T8	301046
CD8	PE-Cy5	Biolegend	RPA-T8	301010
CD8	AlexaFluor700	Biolegend	RPA-T8	300518
CD8	AlexaFluor700	Thermo Fisher	OKT8	56-0086-82
CTLA-4	PE-Dazzle594	Biolegend	L3D10	349922
CX3CR1	PE-Cy7	Biolegend	2A9-1	341612
CXCR1	PE-Cy7	Biolegend	8F1/CXCR1	320620
CXCR3	AlexaFluor488	Biolegend	G025H7	353710
CXCR6	APC	Biolegend	K041E5	356005
CXCR6	PerCP-Cy5.5	Biolegend	K041E5	356010

The liver shapes CD4⁺ T cells

FOXP3	PE	Thermo-Fisher	PCH101	12-4776-42
FoxP3	BV421	Biolegend	206D	320124
GATA-3	BV421	Biolegend	16E10A23	653813
Antigen	Fluorochrome	Manufacturer	Clone	Catalogue Number
GATA-3	BB700	BD Biosciences	L50-823	566643
HLA-DR	FITC	BD Biosciences	G46-6	555811
HLA-DR	BV421	Biolegend	L243	307636
HLA-DR	Horizon V500	BD Biosciences	G46-6	561224
Integrin β 7	PE	Biolegend	FIB504	321204
KLRG-1	PE	Biolegend	SA231A2	367712
PD-1	PE	Biolegend	EH12.2H7	329906
ROR γ t	BV650	BD Biosciences	Q21-559	563424
ROR γ t	FITC	BD Biosciences	Q21-559	563621
S1PR1	eFluor660	Thermo Fisher	SW4GYPP	50-3639-41
T-bet	APC	Thermo-Fisher	eBio4B10	50-5825-82
$\gamma\delta$ -TCR	APC-Vio770	Miltenyi Biotec	11F2	130-109-360
Function				
IFN- γ	APC	BD Biosciences	B27	554702
IFN- γ	AlexaFluor700	Biolegend	B27	506516
IFN- γ	Horizon V450	BD Biosciences	B27	560371
IL-10	BV421	Biolegend	JES3-9D7	501421
IL-10	FITC	Biolegend	JES3-9D7	501411
IL-10	PE	Biolegend	JES3-9D7	501404
IL-17A	PerCP-Cy5.5	Biolegend	BL168	512313
IL-17A	BUV605	Biolegend	BL168	512325
IL-2	PE	Thermo Fisher	MQ1-17H12	12-7029-82
IL-2	PerCP-eFluor710	Thermo Fisher	MQ1-17H12	46-70290-42
IL-2	BB700	BD Biosciences	MQ1-17H12	566406
IL-21	PE	Biolegend	3A3-N2	513004
IL-21	PE	BD Biosciences	3A3-N2.1	562042
IL-4	PE-Cy7	Biolegend	MP4-25D2	500824
IL-4	AlexaFluor647	Biolegend	MPA-25D2	500818
Ki-67	PB	Biolegend	Ki-67	350512
TGF- β	APC	Novus Biologicals	1D11	IC420A
TNF- α	eFluor450	Thermo Fisher	MAb11	48-7349-42
TNF- α	FITC	BD Biosciences	MAb11	554512
TNF- α	PE-Cy7	Biolegend	Mb11	502930
HLA-haplotyping				
HLA-A2	FITC	BioRad	BB7.2	MCA2090
HLA-A2	PE-Cy7	Biolegend	BB7.2	343302
HLA-A3	PE	Thermo Fisher	GAP.A3	11-5754-42
HLA-A9	APC	Miltenyi Biotec	Rea127	130-099-540

The liver shapes CD4⁺ T cells

Supplementary Table 4 – Disease aetiology for functional experiments

Figure	Cytokine	Condition	n=	Breakdown
4A	IL-2	Anti-CD3/CD28	27	2 PBC, 5 control donor, 12 CRC, 1 ARLD, 1 BCM, 1 PSC, 1 ALD, 1 NASH, 1 PLD, 1 Cryptogenic, 1 Budd Chiari
4B	TNF- α	Anti-CD3/CD28	24	2 PBC, 5 control donor, 11 CRC, 1 PSC, 1 ALD, 1 NASH, 1 PLD 1 Cryptogenic, 1 Budd Chiari
4C	IFN- γ	Anti-CD3/CD28	24	2 PBC, 5 control donor, 11 CRC, 1 PSC, 1 ALD, 1 NASH, 1 PLD 1 Cryptogenic, 1 Budd Chiari
4D	IL-4	Anti-CD3/CD28	18	2 PBC, 9 CRC, 1 PSC, 1 ALD, 1 ARLD, 1 BCM, 1 NASH, 1 PLD, 1 Budd Chiari
4E	IL-17	Anti-CD3/CD28	16	2 PBC, 5 control donor, 3 CRC, 1 BCM, 1 ARLD, 1 PLD, 1 cryptogenic, 1 NASH, 1 Budd Chiari
4F	IL-10	Anti-CD3/CD28	22	2 PBC, 1 NASH, 1 PLD, 1 Budd Chiari, 1 PSC, 5 control donor, 9 CRC, 1 BCM, 1 ARLD
4G	IL-21	Anti-CD3/28	11	9 CRC, 1 ARLD, 1 BCM
S5A	IL-2	PMA/Ionomycin	17	2 PBC, 1 PSC, 1 ALD, 1 ARLD, 7 CRC, 1 BCM, 1 NASH, 1 PLD 1 Cryptogenic, 1 Budd Chiari
S5A	TNF- α	PMA/Ionomycin	16	2 PBC, 2 control donor, 6 CRC, 1 PSC, 1 ALD, 1 NASH, 1 PLD 1 Cryptogenic, 1 Budd Chiari
S5A	IFN- γ	PMA/Ionomycin	19	2 PBC, 2 control donor, 1 PSC, 1 ALD, 1 NASH, 1 PLD 1 Cryptogenic, 1 Budd Chiari, 1 ARLD, 7 CRC, 1 BCM
S5A	IL-4	PMA/Ionomycin	18	2 PBC, 2 control donor, 1 PSC, 1 ALD, 1 NASH, 1 PLD 1 Cryptogenic, 1 Budd Chiari, 1 ARLD, 7 CRC, 1 BCM
S5A	IL-17	PMA/Ionomycin	12	2 PBC, 2 control donor, 1 ALD, 1 NASH, 1 PLD 1 Cryptogenic, 1 Budd Chiari, 1 ARLD, 1 CRC, 1 BCM
S5A	IL-10	PMA/Ionomycin	17	2 PBC, 2 control donor, 1 PSC, 1 NASH, 1 PLD, 1 Budd Chiari, 1 ARLD, 7 CRC, 1 BCM
S5A	IL-21	PMA/Ionomycin	11	2 control donors, 7 CRC, 1 ARLD, 1 BCM
S5B	IL-2	Unstimulated	19	2 PBC, 1 PSC, 1 ALD, 1 ARLD, 9 CRC, 1 BCM, 1 NASH, 1 PLD 1 Cryptogenic, 1 Budd Chiari
S5B	TNF- α	Unstimulated	18	2 PBC, 2 control donor, 1 PSC, 1 ALD, 9 CRC, 1 NASH, 1 PLD 1 Cryptogenic, 1 Budd Chiari
S5B	IFN- γ	Unstimulated	21	2 PBC, 2 control donor, 1 PSC, 1 ALD, 1 ARLD, 9 CRC, 1 BCM, 1 NASH, 1 PLD 1 Cryptogenic, 1 Budd Chiari
S5B	IL-4	Unstimulated	20	2 PBC, 2 control donor, 1 PSC, 1 ALD, 1 ARLD, 9 CRC, 1 BCM, 1 NASH, 1 PLD, 1 Budd Chiari
S5B	IL-17	Unstimulated	11	2 PBC, 8 CRC, 2 control donor, 1 ALD, 1 NASH, 1 PLD, 1 Budd Chiari, 1 cryptogenic,
S5B	IL-10	Unstimulated	19	2 PBC, 2 control donor, 1 PSC, 1 ARLD, 9 CRC, 1 BCM, 1 NASH, 1 PLD, 1 Budd Chiari
S5B	IL-21	Unstimulated	13	2 control donors, 9 CRC, 1 ARLD, 1 BCM
S5C	IL-2/TNF- α /IFN- γ	PMA/Ionomycin	7	2 PBC, 1 PSC, 1 ALD, 1 NASH, 1 PLD, 1 Budd Chiari